

## Author response to comments of referee #1

We'd like to thank reviewer #1 for his answer and appreciate his valuable comments.

(referee comments are printed in *italic*, author responses are printed in blue)

*1. The weakest part of the study was investigation in estimating urine patch locations to avoid assumptions on the uniformity of the source on pasture (by measuring dung pile locations and position of the cows). In applications where bLS is often used in non-uniform sources, it is realized that the detector should be some distance downwind to minimize the impact of non-uniform source on emissions but close enough to resolve horizontal gradient (elevated background concentration, a possible problem in this study).*

We do not really understand this statement. In our view, the estimation of the excreta distribution on a real grazed pasture is, despite the necessary approximations, one of the strength of the present study since this issue is either missing in comparable studies (Bell et al., 2017), artificially forced by distributing urine manually on the pasture (Laubach et al., 2012) or by forcing unrealistically high excreta densities during short experiments (Laubach et al., 2013b). We made dung patch surveys and we applied a robust method to estimate dung patch densities based on visual cow monitoring with camera systems. As pointed out in the manuscript, it is a valid assumption that urine and dung patches are similar distributed on the paddock (P12 L28). Auerswald et al. (2010) also found a similar spatial distribution between urine and dung patches on a low intensity pasture.

We are fully aware that placing a detector further downwind minimizes the impact of a non-uniform source. Nevertheless, as referee #2 also pointed out, the small fields ensured a temporarily high stocking density and hence a good sensitivity of the concentration measurement method. We would loss this advantage if placing the detector further downwind. Additionally, for maintaining two realistic grazing systems over an entire season, it was not possible to keep the animals in smaller paddocks. As we investigated a rotational management, placing the detector further downwind would have resulted in an average emission measurement over multiple paddocks (or differently managed areas). Therefore monitoring the temporal dynamics of the emissions (increase with grazing duration, exp. decrease afterwards) would not have been possible.

However, we realized that the presentation of this issue in the manuscript was not optimal and this may have influenced the referee comment. Therefore we improved the manuscript in this respect (see specific comments below).

### **Detailed comments:**

*For the majority of the minor (mostly language related) comments we followed the referee suggestions. Here only the comments that need an answer are listed.*

*1/15 insert 'maximum of  $x \mu\text{g N-NH}_3 \text{ m}^{-2} \text{ s}^{-1}$  at the end'*

As the maximum emissions at the end of the grazing period varied (mostly due to different grazing duration), we kept the sentence unchanged. The overall maximum flux value is included in the range given in the previous sentence.

*2/5 'about eight times lower' - could not find this in Kupper et al (2015) - re-check citation*

The 'eight times lower' factor was calculated based on the TAN flows in Fig. 4b in Kupper et al. (2015). That figure shows that the relative NH<sub>3</sub> emission of grazing livestock (8.9% of excreta TAN) is 7.6 times lower compared to indoor housing including storage and spreading of manure (67.8% of excreta TAN). This factor was rounded to 'about eight'.

We made the reference more specific to "... model Agrammon (Kupper et al., 2015; see Fig. 4b therein) grazing livestock produces ...".

*2/25 was the model 'WindTrax' by ThunderBeach Scientific - need to cite model*

We did not use the model 'WindTrax' in the present study, but we used the model 'bLSmodelR' as described in Sect. 2.2.4.

*3/10 what was the topography (slope, barriers to flow, etc)*

The field site is generally flat with only a small slope towards South-West. There are no trees or hedges in the main wind sectors. The farm facilities north and south of the experimental field (Fig. 1) are the only barriers to the flow.

*4/12 were pressure and temperature corrections needed, if so give calibration factors*

No temperature or pressure corrections were needed within the given uncertainty range.

*4/12 was light intensity used to filter data, if so, give range*

As mentioned in Section 2.2.3 the miniDOAS measurements were filtered based on the level of light reaching the spectrometer. This led to a data rejection rate between about 1 % and 4 % for the different instruments.

*5/3 describe the model, and what modifications were made to Flesch's model, what was different*

We added a reference to Häni et al. (2018) in Sect. 2.2.4, which has been published in the meantime (during the discussion phase). The model characteristics and the minor modifications to Flesch's original model are described there. Additionally we provided more details on the model. The applied model 'bLSmodelR' itself was already used in other publications for NH<sub>3</sub> emission on pastures (Bell et al., 2017). But it has to be noted that we used the model without the newly introduced deposition module.

*5/15 however, the 'underlying' assumption of homogeneity of the emitting surface is less true with increased distance between the source and detector, please include this - it is unclear why the bLS model was not run in its entirety*

We are not sure whether we fully understand this referee comment. We measured close to the emitting surface (pasture paddock) and the pasture field has a generally small variability concerning the surface roughness (as reported by Felber et al., 2015, for the same site). The bLS model was run with a model domain of 250 m length, hence much larger compared to the actual emitting paddock. This has been clarified in the revised manuscript.

*5/25 state the given NH3 concentration certification*

The NH<sub>3</sub> percentage in the gas mixture had a relative uncertainty of 2%, i.e. the NH<sub>3</sub> mixing ratio was 5% ± 0.1%. We added this information in the manuscript.

*5/31 'this is not necessarily the case' - this deserves further comment*

We changed the sentence to: "On a pasture cows can move freely and therefore the urine and dung patches may not be homogeneously distributed on the entire area, which can lead to error prone emission estimates (Auerswald et al., 2010; Bell et al., 2017; Laubach et al., 2013a)."

*6/1 top page 11 states urine patches are the most important factor - then two ways of trying to estimate where these patches exit is tried by GPS of the dung piles and by locating the position of the cows - this cannot be direct emission map of ammonia since cows do not necessarily defecate and urinate at the same location, and the position of the cow adds little information to estimate urine patches.*

The spatial density distribution of urine and dung patches are not identical but very similar on a pasture (Auerswald et al., 2010). The miniDOAS line sensors integrate over a sufficient number of dung and urine patches, but measurement footprint only covers a part of the oblong paddocks. On some stages of the grazing season we could identify clear density gradients along the main paddock axis (see Fig. 3 in the revised manuscript) with a generally high linear correlation between the distributions of dung and cow positions on the pasture. ( $R^2=0.98$ , see P11 L2). The fitted linear regression was used to estimate missing dung distributions and hence estimate the urine patch distribution for certain rotations.

We added a more detailed description (incl. equations) of the procedure in the method section 2.4, and added the new Fig. 3 to illustrate the applied method. Fig. 3a (formerly Fig. 9) was modified, and Fig. 3b shows the regression between parallel surveys of density anomalies for dung patches and cow positions.

*6/7 it is not clear that the error would be reduced by compounding the errors in locating the urine patches, as opposed to assuming a uniform distribution, especially when the uniform criteria declines in importance with some distance downwind.*

As mentioned in the previous comment, we are quite sure that the information on the dung distribution can be used to estimate the distribution of the urine patches. As explained in the response to Comment 1 (see above), we could not have placed our sensors further downwind as we would have lost the possibility to observe the temporal behavior of the emissions as well as the sensitivity of the method (increase in concentration downwind of the paddock).

*7/27 need to expand by providing information on what was done regarding the bLS footprint*

This sentence was misleading because the bLS footprint was not directly used in the flux calculation. We rephrased the sentence to:

"The field scale fluxes were determined based on the concentration differences of the paired MD systems and the dispersion coefficient  $D$  (see Eq. 1) computed by the bLS model."

*7/31 is this 50-70 hours per week?*

As shown in the referenced Table 1, the 50–70 hours correspond to the grazing duration on the investigated paddocks X.11 and X.12 per individual rotation.

*1/8 what is a 'strong' data filter - need to rewrite*

We rephrased the sentence and referred to the data filtering criteria described in Sect 2.2.3.

*8/8 explain where the value '2.54' came from*

We rephrased this paragraph to clarify the issue (see also response to Comment 1 of Referee #2). Because of the low amount of available nighttime data, it was not possible to derive default emission curves for longer nighttime gaps (as shown for daytime conditions in Fig. 6 in the revised manuscript). Thus it was assumed that the general temporal pattern is similar to daytime conditions but with a lower amplitude for nighttime. The corresponding reduction factor (= 0.39, corresponds to the inverse of the original factor 2.54) was based on the overall ratio between mean nighttime and daytime emissions during grazing.

*8/17 are you saying that your design, at specific wind directions, caused an interference of the incoming concentration (upwind) measurement which lead to an under-estimate of emissions - why not filter out the estimates?*

We cannot filter out those periods, as the investigated paddocks were part of an intensive rotational grazing system. This means upwind grazing took place frequently after grazing on the investigated paddocks between the miniDOAS systems. Filtering out those periods would lead to an unacceptable data loss. Additionally the interference effect is relatively small as shown in Fig. 7 (grey line) and Fig. 8 (red boxes). We also presented a way to correct for this effect (P9 L30 - 34). The interference effect has to be considered as a small disadvantage of our experimental design, which was optimized to fulfill several other requirements (see discussion in Section 3.6).

*9/3 use 'recorded' not 'retrieved'*

As the cumulative emissions are also based on gap filled data, we think 'recorded' is not suitable here. Therefore we kept it unchanged.

*9/4 use 'greatest air temperature' and 9/5 'greater emissions'*

After consulting a native English speaker, we kept 'highest' instead of 'greatest'.

*9/6 neither grazing duration nor N input is found in Table 3 - where are these data?*

Table 3 provides information on N input (separated into N excretion total and N excretion urine). Grazing duration can be found in Table 1. We referred to Table 1 for grazing duration in the revised manuscript.

*10/10 usually as an alternative to mass flow controller, the entire tank is weight before and after, was this done in this study?*

We did not weight the tracer gas cylinder before and after the releases. But we used a sophisticated mass flow controller and checked its performance by measuring the individual orifices as described at P11 L14–16.

*10/16 do you mean 'air pressure'*

No, we mean the pressure within the tube of the artificial source system (between the gas tank and the flow controller). We rephrased to '...During that particular release the dynamic pressure within the tubes of the system upstream of the flow controller ...'.

*10/16 don't understand the set-up, what was no longer air tight - needs clarification, also need to indicate why air pressure is involved in recovery*

Similar to the previous answer, we did not mean air pressure but the pressure within the tracer gas tubing system. However, the proposed possible explanation for the high recovery rate in the first gas release trial was purely hypothetical. For clarity reasons we removed it from the manuscript and state that we have no conclusive explanation for this individual result.

*10/19 'an unknown major error source is unlikely' - what does this mean, if unknown how can it be unlikely, delete this sentence as it adds no information - were the results used to correct the emission or was it used to characterize the data? How sure are you that the difference was systematic, if this is important there needs to be a t-test done and if different then an accuracy analysis performed to break the difference into systematic, random and slope errors*

We agree with the referee that the mentioned sentence is not useful and therefore deleted it. With the artificial source we intended to test the applied methodology against a controlled source in an exemplary way, and it was not intended for a calibration or quantitative correction of the measurements. This was clarified in the revised manuscript.

As the artificial source experiments resulted in an average recovery rate that was not significantly different from 100 % ( $111 \% \pm 18 \%$ ) we assume that the used methodology (bLS dispersion modelling, concentration measurements with miniDOAS line sensors) was suitable for quantification of the pasture emissions. If there exist minor systematic errors in the methodology (within the achieved uncertainty range, see Section 3.3.1), they are supposed to be very similar for both parallel pasture systems, and therefore do hardly affect the detection of differences between the two pasture systems (see P12 L17-19, P13 L27-29).

*11/11 how was this correction done in all systems except system G rotation2, needs clarification - also need to document what this means for this latter value that was not corrected*

We are aware that the presentation of this correction procedure was not clear enough. We modified and enhanced the corresponding method section 2.4. More details are given in the response to Referee#2 (Comment 4). We also added the individual uncertainty ranges for the single rotations in the modified Fig. 10.

*11/11 use 'greater uncertainty'*

After consulting a native English speaker, we left the expression unchanged.

*12/3 cited reference not listed*

The cited reference to Móríng et al. (2016) was listed correctly (P17 L5) in the discussion paper.

*13/6 delete 'under real practice conditions'*

We kept the sentence unchanged as previous studies on ammonia emissions (e.g. Laubach et al., 2012, 2013) were often not performed under realistic pasture conditions or included manual (artificial) application of urine to the soil.

## Author response to comments of referee #2

We'd like to thank reviewer #2 for his answer and appreciate his valuable comments.

(referee comments are printed in *italic*, author responses are printed in blue)

*1. The methodology used for gap-filling emissions during night-time (and to a lesser extent for wind sectors coming from the surrounding farms) may be questionable. Indeed, the authors assume that night-time fluxes may be gap-filled based on day-time fluxes, but ammonia fluxes are fundamentally based on thermodynamical equilibrium at the surface (gas-liquid and acid-base equilibriums). This means that (1) the surface ammonia concentration is exponentially increasing with surface temperature due to the gas-liquid or Henry equilibrium, and we would hence expect lower emission at night due to lower temperature and hence lower concentration at the surface; (2) similarly, since ammonia fluxes are proportional to a concentration difference between the surface and a reference level, lower turbulent exchanges at night are expected to decrease night-time ammonia emissions. This means that using daytime fluxes amplitude and dynamics may systematically bias the emissions towards higher values. I would recommend a discussion on that point which may include a study on the temperature and  $u^*$  dependency of the ammonia emissions. Authors could refer to e.g. Flechard et al. (2013) for details on ammonia the points raised above.*

We fully agree with the reviewer that the ammonia emission depends on temperature and turbulence intensity and therefore is generally lower during nighttime compared to daytime conditions. We show this effect for the present study in Fig. 5a. We also account for the day-night difference in the gap filling procedure, but there was obviously a misinterpretation by the referee in this respect. Actually, we did not use the daytime fluxes amplitude to gap fill the missing night time fluxes. We only used the shape of the daytime curve (linear increase during grazing and exponential decrease afterwards), but with a significantly reduced amplitude (0.39) during nighttime (see P9 L12-14). This factor was calculated from the ratio of available nighttime and daytime fluxes during the grazing phase. We rephrased Sect. 3.2 to clarify the applied gap filling procedure and better explain the difference between daytime and nighttime cases.

Regarding the discussion about  $u^*$  and temperature dependency, we already included this effects in our discussion and figures (P8 L26-28, P9 L19-21, Fig. 5) in a qualitative way. Due to the similar temporal pattern of  $u^*$  (wind speed) and temperature at the study site and the frequent calm nighttime conditions it is unfortunately not possible (with a high degree of confidence) to disentangle the dependencies further.

We included a reference to Flechard et al. (2013) (P8 L 32) stating why  $\text{NH}_3$  emissions tend to be lower during nighttime conditions.

*2. Reference to the work of Moring et al. (2016) is lacking. In reference to this work, I wonder if considering the source as a mosaic of emission and deposition hot-spots rather than a distribution of emission patches would conceptually change the results presented here. Could the author elaborate on this question?*

There was already a reference to Moring et al. (2016) in the manuscript (P12 L33). But we assume that the referee wanted to point towards the issue of simultaneous emission (from the excreta patches) and deposition (on the remaining pasture area) on the pasture field. In this respect, our measured fluxes represent the effective net  $\text{NH}_3$  flux attributable to the grazing excreta (combination of emission

and re-deposition within the measured paddocks). But it does not include the large-scale background deposition, because the latter would not produce a horizontal concentration difference. Due to conceptual and practical reasons, a partitioning into gross emission and re-deposition was not in the scope of the present study. This would require separate measurements (e.g. by small-scale enclosures) of individual patches and of surrounding depositing surface areas.

We added a paragraph about this issue in the revised manuscript (Section 2.2.4, P 5 L 18 - 23). In this context, we referenced Móríng et al. (2017), where a simplified combination of modelled pasture emission and deposition is presented (while Móríng et al., 2016 only presented a model for urine patch emission).

Concerning the artificial source experiment, the effect of re-deposition is presumably small as the downwind concentration was measured at only 6 m distance from the release line. Nevertheless, there might be a small bias towards lower recovery rates. As Háni et al. (2018) showed with a similar artificial release, but with NH<sub>3</sub> measurements at 15 m distance from the source, the dry deposition near the point sources may be in the range of 10 %. We therefore assume that the error would be smaller in our experiment.

*3. The uncertainty analysis requires more details and especially on the gap-filling of emissions using the standard curve on Figure 5. An example showing a reconstructed emission would be beneficial here. It is difficult also to understand if the uncertainty analysis on gap-filling spans the actual variability in the fluxes shown in Figure 5 (the error-bars in Figure 5 would also need to be explained).*

An example of a gap filled time series (black points = reconstructed half-hourly data) is actually shown in Fig. 7. Our relatively simple gap filling approach is mainly based on interpolation between available data (either direct linear interpolation or with the help of the management related curves in Fig. 6). Therefore, a simple comparison between gap filled and measured data is not possible.

The uncertainty analysis in Fig. 8 is treating the (systematic) uncertainty of the cumulative emission of an individual rotation, and not of half-hourly fluxes. Only the first error source ( $\Delta C_{\text{bias}}$ ) directly results from the systematic errors of the individual measurements. The other relevant error sources in Fig. 8 result from gap filling of missing flux values.

The vertical bars in Fig. 6 indicate the standard deviation of the half-hourly measurements within the 6-hour averaging interval. We added this information in the figure caption. This variability does not represent an uncertainty but rather the variability in time (mainly between different rotations).

*4. The methodology used to derive the dung patches distribution, the way relative deviation of this dung patches is calculated and the way it is used to correct cow based emissions all need clarifications. I think authors should mention previous work on patches emissions by Moring et al. (2016).*

The calibration/validation of the patch emission model in Móríng et al. (2016) was based on an experiment with a defined pattern of artificially applied urine patches by Laubach et al. (2012). Therefore, we do not see how we can relate our assessment of real grazing patch distribution to their work. For other references to work of Móríng et al. (2016) see response to Comment 2.

However, we agree with the referee that our methodology for determining patch distributions and correcting for their effect should have been presented in a better way. In order to achieve this in the revised manuscript, we modified and enhanced Section 2.4 (Cow and excreta distribution monitoring) in the following way:

i) We added a paragraph at the beginning of Sect. 2.4 clarifying the issue of homogenous or uniform source distribution within the paddock area, deviation from that ideal assumption and the effect on the bLS calculation.

- ii) We moved the old Fig. 9 from to this section (new Fig. 3a) and improved it to illustrate the problem of excreta patch density distribution as well as the applied correction approach.
- iii) We added the new Fig. 3b showing the linear relationship between density anomalies for dung patches and cow positions. This supports the use of cow position information in case of lacking dung patch surveys.
- iv) We added to new equations (Eq. 2 and 3) in the second part of Sect. 2.4 describing the density correction factor  $k_d$  and the calculation of the cumulative integral  $\text{NH}_3$  emission  $E_{\text{int}}$  for each rotation.

*5. The description of the artificial source quality would benefit from more details on the homogeneity of the emissions, the pressure and flow rates stability. Some more examples on measured concentration and retrieved emissions during these trials would also be beneficial as these data were not published previously (to my knowledge).*

In the revised manuscript we have included more information on the concentrations (mean+std) and absolute emissions of the individual experiments in Table 4. In addition we have included data on the pressure and flow rate (and their stability) during the release.

*Detailed comments:*

*P4 L7: delete "important" before reference spectrum*

Was changed accordingly.

*P4 L14-20: some details on the meteorological instruments may be useful. Please evaluate also how important may be high frequency losses on  $u^*$  and H with 10Hz acquisition at 2 m above ground.*

Weather parameters like wind speed, precipitation, temperature and barometric pressure were measured with a WXT520 (Vaisala, Vantaa, FL). Global radiation was measured with a pyranometer (CNR1, Kipp&Zonen, Delft, NL). We added this information in Sect. 2.2.2.

High frequency losses on  $u^*$  and H due to the 10 Hz acquisition at 2 m above ground were typically below 5 %.

*P4 L25-30: 44%-49% missing values for low ustar may actually bias the analysis (see major comments)*

See response to Comment 1. The numbers indicated by the referee are total data loss due to wind direction and  $u^*$  filtering. We better specified the individual effects of  $u^*$  filtering (26% and 30% for system M and G) in the revised manuscript (Sect. 2.2.3). Additionally a potential 50% bias in (mainly nighttime) gap filled values is already included in the uncertainty analyses.

*P5 L6: please give number of thousands of trajectory*

We used 25'000 trajectories per line point (2 m apart). We added this information in Sect. 2.2.4 (P5, L4).

*P5 L9: please give units of E, C and D. I would also suggest to explicit the hypothesis behind this equation: actually  $C_{\text{down}} = D \cdot S + C_{\text{up}}$ , where not other nearby sources are assumed.*

We added the units in the text, but we preferred not to change the equation because it directly represents the emission determination in the present study. Additionally the used form is consistent to other publications (Bell et al., 2017; Flesch et al., 2004)



*P5 L15-18: are the two hypothesis of a uniform and continuous distribution and of a random uniform distribution of sources strictly identical for inverse dispersion?*

Since our method is based on line integrating (i.e. line averaging) concentration measurements, we assume that the two hypothesis are equivalent as long as the footprint of the line concentration is large enough to cover a relatively large number of patches (as it was the case here).

*P5 L31: the work from Moring et al. (2016) should be referred to here and after.*

See response to Comment 4 above.

*P6 L4-8: the method used correct the cow-based emissions based on images and GPS needs to be detailed, as suggested in the major comment section.*

We agree. See response to Comment 4 above.

*P8 EQ-2: The meaning of this is unclear.  $\Delta C_{UD}$  and  $D_{up}$  and  $D_{down}$  should also be time dependent. Please clarify. I would suggest rather using  $t$  and  $E_{def}$ ,  $i(t)$  etc.*

We modified the text and the axis labelling in Fig. 6 to clarify that  $t$  used in this equation is not the absolute measurement time but the elapsed time since the end of grazing of the individual upwind paddock  $i$ .

*P9 L11-15: I would suggest showing the concentration inter-comparison figure in a supplementary material.*

The concentrations during the inter-comparison were typically very low at the remote station as the main focus was on retrieving the bias between the instruments. Therefore, we think that a corresponding figure would not provide useful additional information.

*P9 L28: please explain what is a “systemic” uncertainty.*

This is a typo and should be “systematic” uncertainty. We changed it accordingly.

*P10 L2: I am not sure the word “stable” is appropriate here as it may be understood as “stable thermal stratification”.*

We agree and changed the word to “stationary”.

*P10 L7-10: I wonder what is the variability in the release rate between the critical orifice. I also wonder if the atmospheric pressure has an influence on the release rate at 30 minutes but also over short time scales (seconds). Finally, what is the expected (or even recorded) effect of wind speed variations on release rates : would one expect some ventury effects on the release rates?*

See also response to Comment 5 above. We think the Ventury effect is rather small as wind speeds at the height of the orifices (few cm above ground) were usually low. Additionally it would have no influence on the gas release as the mass flow controller would compensate for pressure fluctuations.

*P10 L28-32: It is quite unclear what the “relative deviation of the dung density” really is. I would suggest providing the exact equation.*

See response to Comment 4. We added Eq. 2 in Sect. 2.4.

*P11 L1-3: it is unclear how exactly missing values are obtained from regression analysis. Could the authors elaborate on that?*

See response to Comment 4 above. The regression analysis is illustrated in the new Fig. 3b.

*P11 L6-12: I would suggest giving details on how the uncertainties are aggregated (may be an equation in a supplementary section?)*

See response to Comment 3 above.

*Table 2: I would suggest finding a way to separate more clearly G and M in this table as in Table 3*  
We modified the layout of Table 2 and Table 3 for better readability.

*Table 3: I suggest only proving 1 digit for temperature and none for rainfall.*

We agree with the reviewer and changed the entries accordingly.

*Figure 5: could you specify the meaning of the error-bars. I would also suggest using negative time values on the left.*

The error bars indicate the standard deviation of the measurements within the 6-hour period. We added this information in the figure caption (Fig. 6 in the revised manuscript). We modified the x-axis according to the referee suggestion.

*Figure 8: Could you provide error bars on both released and inverse modelling with measurements. I would also suggest changing one*

We added the uncertainties of the measurements as error bars (Fig. 9 in the revised manuscript).

*Figure 10: Please explicit the term “relative deviation” in the legend.*

We modified the whole figure for better readability. Additionally we inserted a reference to the equation (Eq. 2 and 3) as described in the response to Comment 4 above.

*Figure 11. Please explicit if error bars are standard deviation, standard errors or interquartile*

We included an explanation of the error bars in the figure caption.

#### References:

Auerswald, K., Mayer, F. and Schnyder, H.: Coupling of spatial and temporal pattern of cattle excreta patches on a low intensity pasture, *Nutr. Cycl. Agroecosystems*, 88(2), 275–288, doi:10.1007/s10705-009-9321-4, 2010.

Bell, M., Flechard, C., Fauvel, Y., Häni, C., Sintermann, J., Jocher, M., Menzi, H., Hensen, A. and Neftel, A.: Ammonia emissions from a grazed field estimated by miniDOAS measurements and inverse dispersion modelling, *Atmospheric Meas. Tech.*, 10(5), 1875–1892, doi:10.5194/amt-10-1875-2017, 2017.

Flesch, T. K., Wilson, J. D., Harper, L. A., Crenna, B. P. and Sharpe, R. R.: Deducing Ground-to-Air Emissions from Observed Trace Gas Concentrations: A Field Trial, *J. Appl. Meteorol.*, 43(3), 487–502, doi:10.1175/1520-0450(2004)043<0487:DGEFOT>2.0.CO;2, 2004.

Häni, C., Flechard, C., Neftel, A., Sintermann, J. and Kupper, T.: Accounting for Field-Scale Dry Deposition in Backward Lagrangian Stochastic Dispersion Modelling of NH<sub>3</sub> Emissions, , doi:10.20944/preprints201803.0026.v1, 2018.

Kupper, T., Bonjour, C. and Menzi, H.: Evolution of farm and manure management and their influence on ammonia emissions from agriculture in Switzerland between 1990 and 2010, *Atmos. Environ.*, 103, 215–221, doi:10.1016/j.atmosenv.2014.12.024, 2015.

Laubach, J., Taghizadeh-Toosi, A., Sherlock, R. R. and Kelliher, F. M.: Measuring and modelling ammonia emissions from a regular pattern of cattle urine patches, *Agric. For. Meteorol.*, 156, 1–17, doi:10.1016/j.agrformet.2011.12.007, 2012.

Laubach, J., Bai, M., Pinares-Patiño, C. S., Phillips, F. A., Naylor, T. A., Molano, G., Rocha, E. A. C. and Griffith, D. W.: Accuracy of micrometeorological techniques for detecting a change in methane emissions from a herd of cattle, *Agric. For. Meteorol.*, 176, 50–63, 2013a.

Laubach, J., Taghizadeh-Toosi, A., Gibbs, S. J., Sherlock, R. R., Kelliher, F. M. and Grover, S. P. P.: Ammonia emissions from cattle urine and dung excreted on pasture, *Biogeosciences*, 10(1), 327–338, doi:10.5194/bg-10-327-2013, 2013b.

Móring, A., Vieno, M., Doherty, R. M., Laubach, J., Taghizadeh-Toosi, A. and Sutton, M. A.: A process-based model for ammonia emission from urine patches, GAG (Generation of Ammonia from Grazing): description and sensitivity analysis, *Biogeosciences*, 13(6), 1837–1861, doi:10.5194/bg-13-1837-2016, 2016.

Móring, A., Vieno, M., Doherty, R. M., Milford, C., Nemitz, E., Twigg, M. M., Horváth, L. and Sutton, M. A.: Process-based modelling of NH<sub>3</sub> exchange with grazed grasslands, *Biogeosciences*, 14(18), 4161–4193, doi:10.5194/bg-14-4161-2017, 2017.

# 1 Ammonia emission measurements of an intensively grazed pasture

2 Karl Voglmeier<sup>1,2</sup>, Markus Jocher<sup>1</sup>, Christoph Häni<sup>3</sup>, Christof Ammann<sup>1</sup>

3 <sup>1</sup>Climate and Agriculture Group, Agroscope, Zürich, 8046, Switzerland

4 <sup>2</sup>Department of Environmental Systems Science, ETH Zurich, Zürich, 8092, Switzerland

5 <sup>3</sup>School of Agricultural, Forest and Food Sciences HAFL, Bern University of Applied Sciences, Zollikofen, 3052, Switzerland

6 *Correspondence to:* Karl Voglmeier (karl.voglmeier@agroscope.admin.ch)

7 **Abstract.** The quantification of ammonia (NH<sub>3</sub>) emissions is still a challenge and the corresponding emission factor for grazed  
8 pastures is uncertain. This study presents NH<sub>3</sub> emission measurements of two pasture systems in western Switzerland over the  
9 entire grazing season 2016. During the measurement campaign, each pasture system was grazed by 12 dairy cows in an  
10 intensive rotational management. The cow herds on the two pastures differed in the energy to protein balance of the diet. NH<sub>3</sub>  
11 concentrations were measured upwind and downwind of a grazed sub plot with line integrating open path instruments that  
12 were able to retrieve small horizontal concentration differences (< 0.2 μg NH<sub>3</sub> m<sup>-3</sup>). The NH<sub>3</sub> emission fluxes were calculated  
13 by applying a backward Lagrangian Stochastic (bLS) dispersion model to the difference of paired concentration measurements  
14 and ranged from 0 to 2.5 μg N-NH<sub>3</sub> m<sup>-2</sup> s<sup>-1</sup>. The fluxes increased steadily during a grazing interval from previous non-  
15 significant values to reach maximum emissions at the end of the grazing interval. Afterwards they decreased exponentially to  
16 near zero values within 3-5 days. A default emission curve was calculated for each of the two systems and adopted to each  
17 rotation in order to account for missing data values and to estimate inflow disturbances due to grazing on upwind paddocks.  
18 Dung and cow location were monitored to account for the non-negligible inhomogeneity of cow excreta on the pasture. The  
19 average emission (± std. dev. of individual rotation values) per grazing hour was calculated as 0.64 ± 0.11 g N-NH<sub>3</sub> cow<sup>-1</sup> h<sup>-1</sup>  
20 for the herd with the N balanced diet (system M) and 1.07 ± 0.06 g N-NH<sub>3</sub> cow<sup>-1</sup> h<sup>-1</sup> for the herd with the protein rich grass-  
21 only diet (system G). Surveys of feed intake, body weight and milk yield of the cow herds were used to estimate the nitrogen  
22 (N) excretion by an animal N budget model. Based on that, mean relative emission factors of 6.4 ± 2.0 % and 8.7 ± 2.7 % of  
23 the applied urine N were found for the systems M and G, respectively. The results can be used to validate the Swiss national  
24 emission inventory and demonstrate the positive effect of a N-balanced diet on pasture NH<sub>3</sub> emission.

## 25 1 Introduction

26 Agricultural livestock production is the main source of air pollution by ammonia (NH<sub>3</sub>) (Bouwman et al., 1997). The largest  
27 share of the emissions is usually assigned to the excretions in the barn with subsequent manure storage and spreading (Kupper  
28 et al., 2015). The high emissions are largely responsible for the formation of secondary aerosols in the atmosphere through  
29 reactions with nitric and sulfuric acids (Nemitz et al., 2009). This can have a significant effect on human health and can also  
30 lead to eutrophication and acidification of the environment through deposition (Sutton et al., 2011).

1 Grazing is considered as one efficient mitigation option to reduce NH<sub>3</sub> volatilisation due to the direct infiltration of urine in  
2 the soil before urea is degraded to ammonium and NH<sub>3</sub>. According to the Swiss inventory model Agrammon (Kupper et al.,  
3 2015; see Fig. 4b therein) grazing livestock produces about eight times lower emissions compared to indoor housing (including  
4 storage and spreading of manure). Emission inventories usually make use of generalized emission factors that relate emissions  
5 to the corresponding source of water soluble nitrogen (urea, ammonium or dissolved NH<sub>3</sub>). In the case of grazed pastures the  
6 relevant nitrogen (N) source is urine by animal excretion (Petersen et al., 1998). However the pasture emission factor still has  
7 a large uncertainty because corresponding NH<sub>3</sub> emission experiments are rare and the available studies reported a large range  
8 of emission factors (5 to 25.7 % of excreted urine N; e.g. Jarvis et al., 1989; Bussink, 1992; Laubach et al., 2012, 2013b).  
9 Many of the studies used manual applied urine and measured the emissions with chamber or wind tunnel methods. These  
10 techniques might lead to questionable results due to the altering of the environment and the high heterogeneity of the emissions  
11 (Misselbrook et al., 2005; Sintermann et al., 2012).  
12 Volten et al. (2012) introduced a new open path miniDOAS system that measures line integrated NH<sub>3</sub> concentrations with a  
13 relatively high temporal resolution. Sintermann et al. (2016) adopted and further developed the system to field applicability  
14 and suggested that paired miniDOAS systems in combination with a dispersion model can be used to estimate emissions of a  
15 pasture. Bell et al. (2017) estimated the NH<sub>3</sub> emission factor based on miniDOAS concentration measurements in combination  
16 with a backward Lagrangian Stochastic (bLS) dispersion model for a 12-d period and demonstrated the applicability of the  
17 miniDOAS / bLS combination for grazing systems. However no information on the excreta distribution on the pasture was  
18 obtained and retrieved emission factors were based on a standard cow and feeding strategy. The relatively short measurement  
19 campaign in May also limited the representativeness of the derived emission factor for a full year. For micrometeorological  
20 methods a spatially homogenous source area is usually needed (Munger et al., 2012) which is often not the case on grazed  
21 pastures (Draganova et al., 2016). However only very few studies reported on the uncertainty associated with a heterogeneous  
22 emission source and those studies usually focused on greenhouse gas emissions (Felber et al., 2015; Peltola et al., 2015).  
23 In the present experiment the miniDOAS systems in combination with bLS modelling were applied to determine NH<sub>3</sub>  
24 emissions of two paired rotational grazing system over a full grazing season. Position monitoring of dung patches with GPS  
25 and of cows with a camera system were used to relate the measured emissions to the animal and excreta density. The calculated  
26 emission factors were based on actual in situ cow productivity data and feed analyses and were compared to standard emission  
27 factors.

## 28 **2 Material and methods**

### 29 **2.1 Site description and experimental design**

30 The study site was located in the Pre-Alps of Switzerland at the research farm Agroscope Posieux in the canton of Fribourg  
31 (46°46'04"N, 7°06'28"E). The soil is classified as stagnic Anthrosol with a loamy texture (20 % clay, 35 % silt and 45 %  
32 sand) and the vegetation consisted mainly of a typical grass clover mixture (10 % to 50 % *Lolium perenne* and 7 % to 40 %

1 *Trifolium repens*) with an increasing clover share during the grazing season. In 2007 the last renovation of the site took place.  
2 Since then the site has been used as an intensive pasture for cattle. Averaged over the past years, the average fertilizer  
3 application rate was about 120 kg N ha<sup>-1</sup> per year, in addition to the excreta of grazing animals. Climate records show an annual  
4 average temperature of 8.7 °C and an annual precipitation amount of 1075 mm (MeteoSwiss, 2018). The experiment was  
5 conducted at a flat 5.5 ha pasture and the cows were managed in a rotational grazing system (Fig. 1). The whole pasture was  
6 divided into two separate systems having different feeding strategies of the cows. The southern system (labeled “G”)  
7 represented a full grazing regime without additional feed supplementation. This resulted in a considerable protein surplus for  
8 the animals leading to an unnecessary high N excretion. At the northern system (labeled “M”) cows were provided with  
9 additional maize silage (roughly 25 % of the total feed dry matter intake) which has a low protein content and resulted in a  
10 more demand-adjusted optimized protein content in the diet (Arriaga et al., 2010; Yan et al., 2006) leading to less N excretion.  
11 Each of the two pasture systems was divided into 11 paddocks resulting in a full rotation period of about 20 days, depending  
12 on the grass growth conditions. The size of the paddocks were adjusted to the different treatments: 1700 m<sup>2</sup> for the northern  
13 M system and 2200 m<sup>2</sup> for the southern G system. The grazing rotation was synchronous for the two systems and started in  
14 the middle of the fields (on paddocks X.11 with X indicating both fields) in westerly direction (until paddock X.16) and then  
15 from the middle (X.21) to the eastern side of the field (X.25). Twice a day (around 05:00 – 07:00 and 15:00 – 17:00 LT) the  
16 cows were brought to the nearby barn for milking. However, in cases of high air temperatures in August and beginning of  
17 September the cows spent a longer period in the barn during daytime (typically 11:00 – 17:00 LT). Due to dry periods during  
18 the summer month and subsequent low grass growth additional pasture areas were used for grazing. The herd for each system  
19 consisted of 12 dairy cows. The main measurement campaign took place between May and October 2016, and in summary,  
20 seven full grazing rotations took place in that period (Table 1). During the measurement campaign, the site was fertilized with  
21 ammonium nitrate (28 kg ha<sup>-1</sup>, end of June) and urea (42 kg ha<sup>-1</sup>, X.11–X.16 mid of August, X.21–X.25 beginning of  
22 September).

## 23 **2.2 Ammonia emission measurements**

### 24 **2.2.1 Ammonia concentration**

25 Line-integrated NH<sub>3</sub> concentrations were measured using four miniDOAS systems (Sintermann et al., 2016). These open path  
26 instruments make use of the differential optical absorption in the UV range (200 – 230 nm). Two miniDOAS systems (namely  
27 MD5 and MD2, naming based on serial number) were installed at system M and two instruments (MD1 and MD6) on system  
28 G (Fig. 1a). All instruments were installed at a height of 1.3 m. Each miniDOAS pair (e.g. MD5 and MD2) was separated by  
29 a horizontal distance of about 30 m which allowed for concentration measurements upwind and downwind of a subplot of the  
30 paddocks in between. The single light path between the sensor and the retroreflector for the individual devices had a length of  
31 30 to 35 m. The instruments reported NH<sub>3</sub> concentration at a temporal resolution of one minute. The one minute data were  
32 processed to 30-min averages for further processing. Due to the predominant wind directions NE and SW one miniDOAS

1 usually reported upwind concentration  $C_{\text{Upwind}}$  ( $\mu\text{g NH}_3 \text{ m}^{-3}$ ) and the other one the downwind concentration  $C_{\text{Downwind}}$  (Fig. 1).  
2 This setting allowed for the computation of the horizontal concentration gradient  $\Delta C$  caused by emissions from the area in  
3 between. The reference spectrum (Sintermann et al., 2016) for each miniDOAS was determined during a seven day inter-  
4 comparison campaign at the Chaumont, Switzerland ( $47^\circ 02' 58'' \text{N}$ ,  $6^\circ 58' 16'' \text{E}$ , 1136m, 20-27 July 2016). The site is located  
5 30 km north-west of Posieux and is only marginally contaminated by  $\text{NH}_3$  and was therefore ideal to compute the reference  
6 spectra. The miniDOAS systems were operated in parallel and compared to wet chemical impingers (Häni et al., 2016) in order  
7 to retrieve the instrumental offset and absolute concentration.

## 8 **2.2.2 Turbulence and meteorological parameters**

9 For the characterization of turbulent mixing the three dimensional wind velocity ( $u$ ,  $v$ ,  $w$ ) and air temperature was measured  
10 at 10 Hz using an ultrasonic anemometer-thermometer (HS-50, Gill Instruments Ltd., UK, hereafter termed sonic anemometer)  
11 mounted on a horizontal arm at 2 m above ground. Each system was equipped with one of those anemometers. The  
12 micrometeorological parameters friction velocity ( $u_*$ ,  $\text{m s}^{-1}$ ), roughness length ( $z_0$ , m) and the Obukhov length ( $L$ , m) were  
13 computed from the 30 min processed eddy covariance data of the sonic anemometer. Further weather parameters were  
14 measured with a standard automated weather station (Campell Scientific Ltd., UK). It used a WXT520 (Vaisala, Vantaa, FL)  
15 to measure wind speed, precipitation, temperature and barometric pressure and a pyranometer (CNR1, Kipp&Zonen, Delft,  
16 NL) to measure global radiation. The station was installed at system M next to the sonic anemometer.

## 17 **2.2.3 Data filtering**

18 The raw MD concentrations were filtered based on the level of light reaching the spectrometer. This led to a data loss between  
19 about 1 % and 4 % for the different MD. An additional filter was applied to account for conditions with low turbulence by  $u_*$   
20 filtering. As the measurement site is located at the Swiss western plateau which is known for low wind speeds especially during  
21 the night a  $u_*$  threshold of  $0.05 \text{ m s}^{-1}$  was applied leading to a relative data loss of 26 % and 30 % for system M and G,  
22 respectively. Flesch et al. (2014) stated that using a  $u_*$  value of  $0.05 \text{ m s}^{-1}$  can be accepted as the data quality does not increase  
23 too much by applying higher  $u_*$  values. The wind sectors facing towards the farm buildings north and south of the fields were  
24 removed as well due to unwanted advection from the nearby farm buildings (Figs. 1 and 2). Filtering for  $u_*$  and wind direction  
25 decreased the data by about 44 % and 49 % for system M and G, respectively.

## 26 **2.2.4 Emission calculation based on dispersion modelling**

27 The emissions were calculated based on inverse dispersion modelling and measurements of  $\text{NH}_3$  concentrations upwind and  
28 downwind of an emitting source. An open-source version of the bLS model by Häni (2017) (based on Flesch et al., 2004)  
29 programmed in the statistical software R (R Core Team, 2016) was used. The first-order bLS model assumed horizontally  
30 homogenous and vertically inhomogeneous Gaussian turbulence and used the Monin-Obukhov Similarity Theory to calculate  
31 the vertical profiles of wind speed and turbulence. Minor adjustments to the original model (Flesch et al., 2004) are described

1 in Häni et al. (2018). The newly introduced deposition module, which is part of the software package, was not used in this  
2 study. The bLS model related the measured 30-min concentration difference  $\Delta C$  ( $\mu\text{g NH}_3 \text{ m}^{-3}$ ) to the unknown emission rate  
3  $E$  ( $\mu\text{g NH}_3 \text{ m}^{-2} \text{ s}^{-1}$ ) of the investigated paddocks (Eq. 1). The coefficient  $D$  ( $\text{s m}^{-1}$ ) was determined based on the simulated  
4 movement of 25'000 fluid particles released at the location of the concentration sensor line and tracked backwards in time up  
5 to a distance of 250 m (extending well beyond the investigated pasture fields). Simulated touchdowns inside the specified  
6 source area contribute to the magnitude of  $D$ .

$$8 \quad E = \frac{C_{\text{Downwind}} - C_{\text{Upwind}}}{D} \equiv \frac{\Delta C}{D} \quad (1)$$

9  
10 The bLS model used wind and turbulence information measured by the sonic anemometer. In order to calculate a concentration  
11 footprint for each 30-min period  $\Delta t$ , averaged data of the wind direction, the standard deviations of the wind components,  $u_*$   
12 and values representing the surface roughness were used. Additional geometric information of the source area locations and  
13 extensions and the position and height of the miniDOAS measurement paths were provided as well. An intrinsic assumption  
14 of the bLS model approach is that the model domain has a uniform surface roughness, which is supported by the results of  
15 Felber et al. (2015) for the same site, and that the defined emitting area is homogenous concerning its source strength. Thus it  
16 is assumed that the monitored pasture paddocks are homogeneously grazed and the urine and dung patches, representing the  
17 main  $\text{NH}_3$  emission sources, are more or less uniformly (or randomly) distributed on the paddock area.

18 The present inverse dispersion method yields a net  $\text{NH}_3$  flux of the investigated paddocks that is in excess of any general  
19 background flux (e.g. due to deposition of ambient  $\text{NH}_3$ , e.g. M3ring et al. (2017)). The resulting flux thus represents the effect  
20 (emission) of grazing excreta. However, because the excreta patches only cover a small part of the grazed pasture, the measured  
21 net flux may also include some short-range re-deposition of the gross excreta  $\text{NH}_3$  emission. A partitioning of these effects is  
22 beyond the scope of the present study and would require small-scale spatially resolved measurements (e.g. by enclosures) of  
23 patch and non-patch surface areas.

### 24 2.2.5 Artificial release experiment

25 In order to test the used methodology an additional experiment with an artificial gas release was conducted in June/July 2017  
26 at the field site next to the sonic anemometer of system M. The source consisted of a grid of 14 critical orifices (100 $\mu\text{m}$   
27 diameter, stainless steel, LenoxLaser, USA) which were installed on ground facing upward with a distance of each other of 2  
28 m. The center of the line was connected to a distribution unit which regulated the gas flow with a mass flow controller (red-y  
29 smart controller, Voegtlin Instruments, Switzerland). The flow rate, pressure within the grid and the accumulated gas flow was  
30 saved to a hard disk within the housing of the distribution unit. A gas mixture with  $5 \pm 0.1 \%$   $\text{NH}_3$  in 95 %  $\text{CH}_4$  (CarbaGas,  
31 Switzerland) was used with a release rate of about 3.1 standard  $\text{L min}^{-1}$ . Two miniDOAS systems (MD2 and MD5) were



1 installed in parallel roughly 6 m north east and south west of the source line to account for the predominant wind directions.  
2 Both instruments were installed at a height of about 0.6 m due to the close distance to the artificial source.

### 3 **2.3 Estimation of N excretion on the pasture**

4 The  $\text{NH}_3$  emission flux, quantified as described above, is a pasture area related quantity. In order to allow a comparison of the  
5 results of the present study with literature reports and with emission inventory models, emission factors were derived by  
6 relating the measured emissions to the urine N input from the cows. As N input to the pasture cannot easily be measured total  
7 N and urine N of the excretions of the cows were estimated with a dairy cow nitrogen budget model based on the official Swiss  
8 feeding recommendation for dairy cows (Bracher et al., 2011). Input to the model were information concerning the milk yield  
9 and N content, the weight of the cows, the calving date, and the crude protein proportional to the N content in the forage (Table  
10 2). Milk yield and body weight was measured for each cow on a daily basis whereas data on grass protein was only collected  
11 and analyzed eight times between end of April and end of September, but usually close in time to the measurement period.  
12 The grass parameters of the systems M and G were averaged for further processing. Crude protein of the maize silage was  
13 analyzed three times (beginning of May, mid of July, beginning of September). Missing data were linearly interpolated between  
14 the measured values. The N in the excretions were finally calculated as a balance between the N input of the feed, N storage  
15 due to body weight gain and N in milk and excreta for each cow and each day of the year. The break-down in urine N and  
16 dung N is based on N balance studies (Bracher et al., 2011). Finally, based on the grazing duration the urine N input to the  
17 investigated paddocks was computed for each rotation. An associated uncertainty of 15 % was estimated by comparing the N  
18 budget model to published results of Swiss N excretion studies (Bretscher, unpublished data).

### 19 **2.4 Cow and excreta distribution monitoring**

20 The measured concentration difference and thus the derived  $\text{NH}_3$  flux is mainly related to the emission of the surface area  
21 between the MD sensor paths on each grazing system (according to the main wind directions, Fig. 1). This is only a part of the  
22 entire paddock area, which was considered as uniformly emitting area in the bLS calculations (Sect. 2.2.4) and for which the  
23 average urine N input was quantified (Sect. 2.3). On a pasture cows can move freely and therefore the urine and dung patches  
24 may not be homogeneously distributed on the entire area, which can lead to error prone emission estimates (Auerswald et al.,  
25 2010; Bell et al., 2017; Laubach et al., 2013a).

26 In order to assess the spatial distribution of the cow excreta on the paddocks X.11 and X.12 as main emission sources in our  
27 experiment, we used two different approaches. The number and position of dung patches was determined with a hand held  
28 GPS device within the first 3–5 days after grazing. In addition, the cow position on the pasture was monitored with a day–  
29 night digital camera system at a temporal resolution of 10 minutes. The location of the individual cows were manually marked  
30 on the displayed pictures in a post processing step. However, the night mode often did not yield useful information and  
31 therefore images showing the cow positions during nighttime were very sparse.

1 In order to account for inhomogeneity of the excreta distribution within the investigated paddocks, they were divided as shown  
 2 in Fig. 3a. The middle sections between the paired MD sensor paths represent the main source areas of the measured fluxes.  
 3 Their excreta density  $d_{X.meas}$  was related to the density of the entire paddocks  $d_{(X.11+X.12)}$  to determine the excreta density  
 4 correction factor  $k_d$ :

$$5 \quad k_d = \frac{d_{(X.11+X.12)}}{d_{X.meas}} \quad (2)$$

6 The exemplary dung patch survey in Fig. 3a shows a positive deviation from the average paddock-wide density for both system  
 7 M ( $k_d = 1.28$ ) and system G ( $k_d = 1.40$ ). However, dung observations were only available for two rotations for the paddock  
 8 M.11, three rotations for G.11 and two rotations for X.12 while daytime cow position observation by camera was available for  
 9 the whole measurement campaign for system M, and from rotation three onwards for system G. As cow excreta (mainly in  
 10 form of urine) is the main source of  $\text{NH}_3$  emissions, missing dung density values were estimated based on a regression analysis  
 11 ( $R^2 = 0.98$ ) between parallel surveys of density anomalies for dung patches and cow positions (Fig. 3b).

12 The  $k_d$  factors derived from the combined information of the dung patch and the cow position surveys were used to calculate  
 13 integral  $\text{NH}_3$  emissions  $E_{int}$  for each rotation for the two investigated paddocks X.11 and X.12 (with corresponding areas A)  
 14 for a time period between start of grazing until end of grazing (EOG):

$$15 \quad E_{int} = \sum_{t=start\ of\ grazing}^{EOG+10\ days} E(t)\Delta t \cdot k_d^{-1} \cdot (A_{X.11} + A_{X.12}) \quad (3)$$

### 19 3 Results and Discussion

20 This chapter is organized as follows. The first section (Sect. 3.1) shows the observed  $\text{NH}_3$  concentrations during the grazing  
 21 campaign, whereas the next sections present and discuss the emission fluxes. Sect. 3.2 describes the measured area-related  
 22 fluxes including interference correction and the gap filling leading to cumulative emissions over individual grazing events.  
 23 The corresponding emission uncertainty and its sources are discussed in Sect. 3.3. The area related emission were converted  
 24 to animal related emissions using cow and dung distribution monitoring results (Sect. 3.4) and further converted to emission  
 25 factors related to animal urine N (Sect. 3.5). In the final section of the chapter (Sect. 3.6) the advantages and problems of the  
 26 experimental design are highlighted.

27

### 1 3.1 Ammonia concentrations during grazing season

2 The  $\text{NH}_3$  concentration values observed during the entire measurement campaign had a strong temporal and spatial variability.  
3 They were typically in the range of 4–15  $\mu\text{g NH}_3 \text{ m}^{-3}$  with maximum values of about 100  $\mu\text{g NH}_3 \text{ m}^{-3}$ . As shown in Fig. 2 the  
4 highest concentrations usually resulted from advection from the nearby farm located in the northern direction of the miniDOAS  
5 instruments. This advection is weaker at the southern system G due to the larger distance to the farm. The general concentration  
6 pattern is nevertheless very similar for both systems. The highest wind speeds (above 4  $\text{m s}^{-1}$ ) usually resulted in low  $\text{NH}_3$   
7 concentrations due to a good mixing of the atmospheric boundary layer with lowest concentrations coming from the south–  
8 western direction. The higher background concentration from the north–easterly direction is probably a result of a nearby  
9 piggery some 350 m away. During the whole measurement period (beginning of May – mid of October) the MD instruments  
10 were online between 62 % (MD 6) and 85 % (MD 2) of the time. Power failure and instrument errors were the main reasons  
11 for the partial data loss. The measurement campaign at the Chaumont mountain site (Sect. 2.2.1) led to a data loss for the first  
12 three days during rotation four. During rotation one no data of the MD instruments MD1 and MD6 could be acquired due to  
13 instrument errors.

14 During the grazing period on the paddocks X.11 and X.12 the  $\text{NH}_3$  concentration difference increased (see example for one  
15 rotation in Fig. 4) due to increased excreta on the field, mainly in the form of urine. Concentration differences in the range of  
16 about 0 – 8  $\mu\text{g NH}_3 \text{ m}^{-3}$  for system M and of about 0 – 15  $\mu\text{g NH}_3 \text{ m}^{-3}$  for system G were measured. A few hours after grazing  
17 the concentration differences started to decrease significantly. Mostly within the first three to five days after the EOG the  
18 concentration differences reached values around the accuracy limit of the MD devices (about 0.2  $\mu\text{g NH}_3 \text{ m}^{-3}$ ). Typically for  
19 the Swiss western plateau wind speed had a strong diurnal pattern with low wind speeds during nighttime. This often led to a  
20 weak mixing in the boundary layer and subsequent high observed concentrations. In order to avoid error prone emission  
21 estimates the concentration values were filtered according to Sect. 2.2.3. This led to low data availability for emission  
22 calculation especially during nighttime conditions. Precipitation events typically resulted in low concentrations and subsequent  
23 low concentration differences.

### 24 3.2 Field scale fluxes

25 The field scale fluxes were determined based on the concentration differences of the paired MD systems and the dispersion  
26 coefficient  $D$  (see Eq. 1) computed by the bLS model. The emissions typically showed a diurnal emission pattern with highest  
27 values occurring between midday and late afternoon, which correlated well with atmospheric driving parameters like air  
28 temperature, wind speed and global radiation (Fig. 5, horizontal axis). This emission behaviour can theoretically be explained  
29 with higher wind speeds and unstable conditions during daytime leading to a reduction of the aerodynamic resistance at the  
30 interface between the atmosphere and the urine patch surface and thus leading to higher emissions. Ammonia fluxes are also  
31 based on the thermodynamic equilibrium at this interface leading to higher emissions with increasing temperatures during  
32 daytime (Flechard and Sutton, 2013). Beside the diurnal variation, the emissions generally increased during the grazing phase

1 (typical grazing duration: 50-70 hours, Table 1) with a fast subsequent decrease afterwards (Fig. 5a, vertical axis). The  
2 observed emission fluxes usually decreased to insignificant values within 3–5 days after EOG. This management related  
3 temporal pattern could be parameterised as shown in Fig. 6, where daytime emission values are plotted against the elapsed  
4 time since the start / end of the grazing period. The emissions showed an approximately linear increase during the grazing (due  
5 to the continuous formation of new excreta patches) and an exponential decay after EOG. The decay or e-folding time of the  
6 exponential function was evaluated as 28 and 23 hours (37 % of maximum value at the beginning) for the systems M and G,  
7 respectively.

8 Due to quality related data filtering (Sect. 2.2.3) and missing concentration data the emission time series had a considerable  
9 share of gaps that needed to be filled in order to calculate cumulative emissions. The following relatively simple gap filling  
10 procedure was applied:

11 (i) Gaps shorter than three hours were filled by linear interpolation between available measurements

12 (ii) For longer gaps during daytime, the management related emission curves in Fig. 6 (linear increase during grazing and  
13 subsequent exponential decrease) were fitted to the available daytime data of individual grazing phases. This allowed to  
14 account for different weather and soil effects between the rotations.

15 (iii) Because of the low amount of available nighttime data, it was not possible to derive and fit individual curves for longer  
16 nighttime gaps. Thus it was assumed that the general temporal pattern is similar to daytime conditions (curves in Fig. 6) but  
17 with a lower amplitude for nighttime. The corresponding reduction factor (= 0.39) was based on the overall ratio between  
18 mean nighttime and daytime emissions during grazing.

19 Due to the limited amount of measured data and the considerable number of possible environmental driving parameters (air  
20 temperature, global radiation, wind speed, precipitation, soil / leaf humidity, Fig. 5, also Bell et al., 2017; Hani et al., 2016;  
21 Laubach et al., 2013b; Moring et al., 2016) the emissions were not parameterised as a function of these parameter but only as  
22 a function of grazing duration and elapsed time since start/end of grazing. Nevertheless, a good agreement was found using a  
23 linear increase of emissions during the grazing period and an exponential decrease afterwards.

24 The applied flux measurement approach as described in Section 2.2 assumes a spatially limited emission between the two  
25 measurement paths and negligible emission upwind of the system. However, upwind paddocks were grazed while the  
26 measurement paddocks were in the emission decay phase. In some cases, depending on wind direction, the emission sources  
27 on the upwind paddocks can lead to a greater concentration signal of the inflow compared to the outflow instrument. They  
28 interfere with the concentration signals of the paddock(s) of interest and can lead to an underestimation of the true emission.

29 In the strict sense this is a problem of an under-determined systems when fewer concentration detectors are available compared  
30 to the emission sources (see also Bell et al., 2017). To estimate the influence of grazed upwind paddocks, a default emission  
31 pattern  $E_{\text{def}}(t)$  according to the fitted curves in Fig. 6 was used. The effect of each upwind paddock  $i$  on the measured  
32 concentration difference  $\Delta C$  in Eq. 1 was calculated from the corresponding bLS dispersion coefficients for both MD systems

33  $D_{i,\text{Upwind}}$  and  $D_{i,\text{Downwind}}$ .

34

$$\Delta C_{\text{corr}} = \sum_i E_{\text{def}}(t_i) \cdot (D_{i, \text{Upwind}} - D_{i, \text{Downwind}}) \quad (4)$$

2

3 This effect was corrected for in the flux calculation (Eq. 1). The resulting measured fluxes during the campaign were within a  
4 range of 0 to 2.1  $\mu\text{g N-NH}_3 \text{ m}^{-2} \text{ s}^{-1}$  for system M and 0 to 2.3  $\mu\text{g N-NH}_3 \text{ m}^{-2} \text{ s}^{-1}$  for system G.

5 The cumulative integral emission  $E_{\text{int}}$  (Eq. 3) for each system and rotation was calculated based on the gap-filled half-hourly  
6 fluxes and the area of the investigated paddocks (see example in Fig. 7). Depending on atmospheric driving parameters (mainly  
7 precipitation) about half of the overall emission occurred during the grazing phase. Precipitation events during that time period  
8 led to a significant reduction in emissions with subsequent higher emission later on (observable especially during rotations  
9 two and the higher fluxes on the 14<sup>th</sup> of May in Fig. 6). Over the entire grazing season, cumulative emissions for the different  
10 rotations were retrieved under variable weather conditions with highest air temperatures recorded during rotation three to  
11 rotation six and the highest precipitation amounts occurring at the first three rotations (Table 3). The highest integral emissions  
12 occurred usually at the southern paddock and showed a strong temporal variability depending mainly on the grazing duration  
13 (Table 1) and N input (Table 3). The emissions during rotation seven on system G showed the largest magnitude of all single  
14 rotations and fields. This is also in line with the highest N input to the pasture from cow excreta.

### 15 3.3 Uncertainty of emission flux measurements

#### 16 3.3.1 Effect of different error sources

17 The performance of the miniDOAS devices for concentration measurements was optimised by adjusting the offsets among all  
18 four instruments during the 7-d inter-calibration at the Chaumont site between rotation 3 and 4. During that period the  
19 instruments were running in parallel and the measured concentrations (mostly 0 – 2  $\mu\text{g NH}_3 \text{ m}^{-3}$ ) were compared to the  
20 measurements of wet chemical impingers. It was found that the potential bias between the instruments was below 0.2  $\mu\text{g NH}_3$   
21  $\text{m}^{-3}$  and was therefore similar to the results by Sintermann et al. (2016).

22 Missing flux data were replaced either by values of the default emission curve (Fig. 6) or by applying a liner interpolation  
23 between measurements. The default emission curves were also used to estimate unwanted interferences in the measured  
24 concentration differences from emitting upwind paddocks. In order to test the sensitivity of the emission result to uncertainties  
25 in the gap filling method and interferences from upwind grazing, we varied the values of the default emission curve to 50 %  
26 and 150 % of the default values. The sensitivity towards the exponential decay time of the default emission curve was tested  
27 with a systematic increase in the decay time of 50 % (decay\_slow) and a reduction of 30 % (decay\_fast). We found (Fig. 8)  
28 that the relative effect of all simulated errors on the cumulative emissions was generally below 20 % for individual rotations  
29 (except for few outliers). The highest impact on the emission results was due to the uncertainty in the gap filling of missing  
30 values that predominantly occurred during night. Since the simulated error sources are independent, they were combined to an  
31 overall measurement related error of 17 % by Gaussian error propagation.

1 The bLS dispersion modelling is a well-defined approach and was evaluated extensively by Flesch et al. (2005), Harper et al.  
2 (2010), and McGinn et al. (2009) who found that the model uncertainty is typically in the order of 20 %. Combining the 20 %  
3 uncertainty for the bLS modelling and the 17 % measurement related uncertainty results in total mean systemic uncertainty of  
4 26 %.

### 5 3.3.2 Artificial gas release

6 For an **exemplary** test of the performance of the applied methodology, **tracer** gas releases were conducted at the same site in  
7 the year after the main experiment in June and July 2017. The gas was only released during **stationary** westerly winds in order  
8 to avoid advection from the nearby barn. Table 4 lists the main meteorological and technical aspects of the individual releases  
9 and shows the corresponding results. The duration of the releases strongly depended on the observed wind speed and varied  
10 therefore significantly.

11 Due to the westerly winds MD 2 detected the upwind concentrations and MD5 the downwind concentrations. All  
12 measurements were averaged to **30-min** values and the emissions were calculated following Eq. 1 (Fig. 9). In order to check  
13 the mass flow controller of the artificial source, the release rate of all single orifices were measured during three releases  
14 (release 2, 4 and 5). The observed differences between the summed orifice release rates and the measured mass flow from the  
15 gas cylinder varied between -7 and 9 % and an overall average of only  $1 \pm 8.7$  %. **The associated uncertainty of the artificial**  
16 **source of 17.4 % was calculated as two times the standard deviation.**

17 The quality of the calculated emission for each source experiment is defined as recovery rate which is calculated as the ratio  
18 of the measured cumulative emissions of the bLS and the cumulative measured emission from the flow controller (Table 4).  
19 Four out of five releases resulted in a recovery rate above 100 % and four release experiments showed a recovery rate between  
20 88 and 124 %. Release number one had an exceptional high recovery rate of about 150 %. During that particular release the  
21 **dynamic pressure within the tubes of the system upstream of the flow controller** was higher **at the beginning** compared to the  
22 following ones. **Nevertheless, we have no conclusive explanation for this individual result.** The overall mean of 111 % and the  
23 standard deviation of 18 % was calculated based on all individual **half-hourly** measurements. **As the recovery rates were not**  
24 **significantly different from 100 % we can assume that the inverse dispersion methodology in combination with miniDOAS**  
25 **line sensors is suitable to quantify the NH<sub>3</sub> emission of the pasture experiment.**

### 26 3.4 Animal related emissions

27 As the bLS approach assumes a homogenous **spatial** distribution of emission sources within the investigated paddock, the  
28 actual distribution of the cow excreta could have a significant influence on the calculated emissions **per animal or per excreta**  
29 **input. The relative density of the emitting urine patches was assumed to be proportional to the observed density of dung patches**  
30 **and/or animal positions as described in Sect. 2.4.** Figure 10 shows the **correction factor  $k_d$**  (Eq. 2, 3) of the **excreta** density in  
31 the main measurement section (between the MD instruments) from the mean density of the entire paddock area. **In case of a**  
32 **uniform excreta distribution  $k_d$  should be 1.** However, a considerable heterogeneous distribution was found for the different

1 rotations and paddocks. On the southern pasture (system G) a generally higher excreta density was found between the MD  
2 devices in comparison to the averaged field. On the northern pasture (system M) the effect was more variable with negative  
3 deviations until rotation 5 and positive deviations towards the end of the grazing season.

4 There is some uncertainty associated to the visual identification (for GPS localisation) of dung patches due to potential double  
5 counting or overlooking of dung patches on the paddock, and due to the use of the linear relationship between cow and dung  
6 density. But these errors are assumed to behave random-like and are thus relatively small resulting in a combined relative  
7 emission uncertainty of about 7 %. This is much smaller compared to the systematic uncertainty of the measured fluxes (Sect.  
8 3.3.1). Since there was no cow nor dung monitoring data available for system G during rotation 2, no correction for  
9 inhomogeneous excreta density was applied in this case, but a higher uncertainty (25 %) was attributed to the emission based  
10 on the variability of the dung density of the other rotations (Fig. 10).

11 In order to calculate the animal related emission and the emission factor for the individual rotations, the derived cumulative  
12 emissions were corrected for excreta inhomogeneity (Eq. 3) by applying excreta density ratios  $k_d$  shown in Fig. 10 (see also  
13 Eq. 2). The measured emissions per cow and grazing hour (h) stayed rather constant with a value of about  $0.64 \pm 0.11$  g N-  
14  $\text{NH}_3 \text{ cow}^{-1} \text{ h}^{-1}$  (mean  $\pm$  one standard deviation) for system M and about  $1.07 \pm 0.12$  g N- $\text{NH}_3 \text{ cow}^{-1} \text{ h}^{-1}$  for system G (Fig. 11).  
15 For comparison, the application of a 10 % standard emission factor for  $\text{NH}_3$  (EMEP/EEA, 2016) results in larger mean values  
16 and a larger variability (system M:  $0.99 \pm 0.24$  g N- $\text{NH}_3 \text{ cow}^{-1} \text{ h}^{-1}$ ; system G:  $1.22 \pm 0.31$  g N- $\text{NH}_3 \text{ cow}^{-1} \text{ h}^{-1}$ ).

17 The error bars in Fig. 11 represent the total error of the absolute emissions. This error is predominantly due to systematic  
18 effects (Sect. 3.3.1) that are identical (bLS uncertainty) or very similar (gap filling uncertainty) for the two parallel pasture  
19 systems. Therefore these systematic errors are not relevant for the comparison of the two systems, for which only the random  
20 uncertainty and the instrument bias uncertainty (Fig. 8) have to be considered. The random uncertainty for the seasonal mean  
21 was estimated from the variability between rotations. In combination with the bias uncertainty this results in a significant mean  
22 difference between the two systems of  $0.43 \pm 0.13$  g N- $\text{NH}_3 \text{ cow}^{-1} \text{ h}^{-1}$ , corresponding to a relative reduction effect of the N-  
23 balanced diet compared to the grazing-only diet of 40 %.

### 24 3.5 Emission factors for the two pasture systems

26 The EF values for individual rotations in Table 3 are based on the measured cumulative emissions relative to the urine N  
27 deposited (excreted) on the two pasture systems for the different rotations. They range within 4.9 % – 11.1 % for system M  
28 and show generally higher values for system G (range 7.2 – 16 %). The highest EF values were observed during the second  
29 rotation. They are mainly driven by the low N content of the grass on pasture resulting in low estimated urine N excretion  
30 (Table 2). The variation in EF is in contrast to the rather stable measured absolute  $\text{NH}_3$  emissions as shown in Fig. 11. This  
31 may indicate that the analysed grass samples are not fully representative for the selective grazing intake of the cows. On the  
32 other hand, an exceptionally high value of the measured emission is unlikely, because a rainfall event started during the second  
33 half of the grazing period and lasted almost two days with a precipitation amount of about 40 mm (data not shown). Typically  
34 smaller volatilisation of  $\text{NH}_3$  is expected during such weather periods (Sommer and Olesen, 2000). A delayed onset of the

1 emissions was observed as described in Möring et al. (2016) after the rain event stopped. However, the emissions were small  
2 compared to the ones observed during the first grazing day (roughly one third) and were therefore not able to counterbalance  
3 the reduced emissions of the second part of the grazing period.

4 The annual average pasture EF and its uncertainty was derived from the overall means of NH<sub>3</sub> emission and urine N input and  
5 resulted in  $6.4 \pm 2.0$  % for system M and  $8.7 \pm 2.7$  % for system G. The uncertainty of about 1/3 mainly stem from the  
6 systematic errors discussed in Sect. 3.3.1 and 2.4. The found mean EFs are ranked towards the lower end of reported values  
7 (5 – 26 % of excreted urine N, e.g. Bussink, 1992; Jarvis et al., 1989; Laubach et al., 2012, 2013b) but are in line with the  
8 results (6 – 9 %) of the recent study by Bell et al. (2017). A single emission factor as used in many inventory models (e.g.  
9 EMEP/EEA, 2016; Kupper et al., 2015) would not be able to reflect the observed difference of 2.3 % between the two  
10 grazing/feeding systems in our experiment. The reduction in EF for system M is not statistically significant but may indicate  
11 a nonlinear effect of the N input rate on the NH<sub>3</sub> emission, similar to the findings of the recent literature synthesis study by  
12 Jiang et al. (2017) who reported a higher emission factor with increasing fertiliser N application. Thus the optimised N-  
13 balanced feeding strategy may decrease the NH<sub>3</sub> emission even more than expected from the reduced urine N excretion.

### 14 **3.6 Advantages and problems of experimental setup**

15 The present field experiment was optimised to measure the NH<sub>3</sub> emissions of two neighbouring pastures managed in an  
16 intensive rotation. The periodic high density of animals (55-70 cows ha<sup>-1</sup>) and fresh excreta on the grazed paddocks resulted  
17 in intermittent high fluxes and allowed to observe the temporal behaviour of the emissions (Fig. 6, Fig. 7). This would not be  
18 possible on a continuous grazing system with much larger paddock sizes and accordingly smaller excreta densities and  
19 emissions. For continuous grazing on large fields other micrometeorological measurement techniques like the eddy covariance  
20 (Ammann et al., 2012) would be preferable. The small paddock sizes in this study also kept the cow excreta heterogeneity on  
21 a moderate level, whereas on larger free range grazing areas the animals often gather at the same place (Cowan et al., 2015)  
22 leading to a more complicated quantification of the EF. While the distribution of dung patches and cows was monitored by  
23 means of visual inspection or evaluation of the camera images, a direct localisation of urine patches was not possible in this  
24 way. Sensors for urine patch detection exist, but are either still in development (Kumar et al., 2016), relatively expensive (Quin  
25 et al., 2016), or unpractically for field scale experiments (Dodd et al., 2015). Therefore we assumed a similar density  
26 distribution of dung and urine patches on the paddock (Auerswald et al., 2010; Luo et al., 2017).

27 The present setup with the parallel pastures and accordingly similar micrometeorological conditions constituted an effective  
28 way to analyse the difference between the two systems as the main systematic uncertainty source of the single pasture emissions  
29 (bLS, Sect. 3.3.1) were cancelled out. However, subsequent grazing on neighbouring upwind paddocks could produce  
30 interferences with the measurements that could be corrected only in an approximate way. Another error source arose due to  
31 the strong variability of the measured crude protein in the grass with consequent high variability of the estimated N in the  
32 urine. It was not directly measured as automated monitoring techniques for urine N on the pasture are not yet mature enough



1 and still have some limitations regarding the animal welfare (Misselbrook et al., 2016). Manual measurements of the urine N  
2 amount were outside of the scope of this project due to the laborious work.

### 3 **4 Concluding remarks**

4 In a paired field experiment NH<sub>3</sub> emissions on two pasture systems were measured for an entire grazing season under real  
5 practice conditions. The herds of the two pastures were kept in an intensive rotational grazing management with different  
6 protein to energy ratios resulting in different N excretion rates. The fast rotation with a short but high stocking rate and excreta  
7 deposition within the grazed paddock allowed to observe the temporal dynamics of the corresponding NH<sub>3</sub> emission. Maximum  
8 emissions were found at the end of each grazing phase on the investigated area. Afterwards an exponential decay of the  
9 emissions led to non-significant low values typically within 3-5 days. A diurnal emission pattern with peaks during the  
10 afternoon was observed on all rotations.

11 Monitoring of the cow and dung density distribution was essential for a quantitative comparison of the two systems. The  
12 emission per cow and grazing hour showed only a very limited variation over the season but a distinct difference (40 %)  
13 between the two systems. About half of this difference could be explained by the different urine N excretion rate of the two  
14 herds. The resulting average EFs were  $6.4 \pm 2.0$  % and  $8.7 \pm 2.7$  % for the herd with the N balanced diet and the herd with the  
15 N surplus in the forage, respectively. Thus the experiment showed the large potential of an optimised feeding strategy to reduce  
16 NH<sub>3</sub> emissions. The results can also serve as a validation for the Swiss national emission inventory for NH<sub>3</sub> emissions on  
17 pastures. It is recommended for further studies to include the regular analyses of the N content in the urine in order to overcome  
18 the associated uncertainties.

19

20 *Data availability.* Data obtained in this study is online available at [doi:10.5281/zenodo.1305180](https://doi.org/10.5281/zenodo.1305180) (Voglmeier et al., 2018).

21

22 *Competing interests.* The authors declare that they have no conflict of interest.

23

24 *Acknowledgements.* We gratefully acknowledge the funding from the Swiss National Science Foundation (Project  
25 NICEGRAS, number 155964). Christoph Häni was additionally supported by the Swiss Federal Office for the Environment  
26 FOEN (06.9115.P2 I 0094-1922) and Karl Voglmeier by a MICMoR Fellowship through KIT/IMK-IFU. We wish to thank  
27 Lukas Eggerschwiler, Robin Giger, Walter Glauser, Harald Menzi, Andreas Mürger and Jens Leifeld for support in the field  
28 and helpful discussions. We especially acknowledge the contribution of Harald Menzi in the design and planning of the  
29 experiment. We are grateful to Albrecht Neftel for the helpful discussions and advise concerning the MiniDOAS  
30 measurements. We thank Daniel Bretscher for the support with the N balance computation of the cows and the discussions of  
31 these data.

32

## 1 **References**

- 2 Ammann, C., Wolff, V., Marx, O., Brümmer, C. and Neftel, A.: Measuring the biosphere-atmosphere exchange of total reactive  
3 nitrogen by eddy covariance, *Biogeosciences*, 9(11), 4247–4261, doi:10.5194/bg-9-4247-2012, 2012.
- 4 Arriaga, H., Salcedo, G., Calsamiglia, S. and Merino, P.: Effect of diet manipulation in dairy cow N balance and nitrogen  
5 oxides emissions from grasslands in northern Spain, *Agric. Ecosyst. Environ.*, 135(1–2), 132–139,  
6 doi:10.1016/j.agee.2009.09.007, 2010.
- 7 Auerswald, K., Mayer, F. and Schnyder, H.: Coupling of spatial and temporal pattern of cattle excreta patches on a low intensity  
8 pasture, *Nutr. Cycl. Agroecosystems*, 88(2), 275–288, doi:10.1007/s10705-009-9321-4, 2010.
- 9 Bell, M., Flechard, C., Fauvel, Y., Häni, C., Sintermann, J., Jocher, M., Menzi, H., Hensen, A. and Neftel, A.: Ammonia  
10 emissions from a grazed field estimated by miniDOAS measurements and inverse dispersion modelling, *Atmospheric Meas.*  
11 *Tech.*, 10(5), 1875–1892, doi:10.5194/amt-10-1875-2017, 2017.
- 12 Bouwman, A. F., Lee, D. S., Asman, W. a. H., Dentener, F. J., Van Der Hoek, K. W. and Olivier, J. G. J.: A global high-  
13 resolution emission inventory for ammonia, *Glob. Biogeochem. Cycles*, 11(4), 561–587, doi:10.1029/97GB02266, 1997.
- 14 Bracher, A., Schlegel, P., Münger, A., Stoll, W. and Menzi, H.: Möglichkeiten zur Reduktion von Ammoniakemissionen durch  
15 Fütterungsmassnahmen beim Rindvieh (Milchkuh), SHL Agroscope Zollikofen Posieux, 2011.
- 16 Bretscher, D.: Background data for Swiss national greenhouse gas inventory, Agroscope, unpublished.
- 17 Bussink, D. W.: Ammonia volatilization from grassland receiving nitrogen fertilizer and rotationally grazed by dairy cattle,  
18 *Nutr. Cycl. Agroecosystems*, 33(3), 257–265, 1992.
- 19 Carslaw, D. C. and Ropkins, K.: openair --- an R package for air quality data analysis, *Environ. Model. Softw.*, 27–28, 52–61,  
20 2012.
- 21 Cowan, N. J., Norman, P., Famulari, D., Levy, P. E., Reay, D. S. and Skiba, U. M.: Spatial variability and hotspots of soil N<sub>2</sub>O  
22 fluxes from intensively grazed grassland, *Biogeosciences*, 12(5), 1585–1596, doi:10.5194/bg-12-1585-2015, 2015.
- 23 Dodd, M., Manderson, A., Budding, P., Dowling, S., Ganesh, S. and Hunt, C.: Preliminary evaluation of three methods for  
24 detecting urine patches in the field, in *Moving Farm Systems to Improved Attenuation*, p. 8, Fertiliser and Lime Research  
25 Centre Palmerston North, NZ., 2015.
- 26 Draganova, I., Yule, I., Stevenson, M. and Betteridge, K.: The effects of temporal and environmental factors on the urination  
27 behaviour of dairy cows using tracking and sensor technologies, *Precis. Agric.*, 17(4), 407–420, doi:10.1007/s11119-015-  
28 9427-4, 2016.
- 29 EMEP/EEA: Air pollutant emission inventory guidebook - 2016, Technical Report, EEA., 2016.
- 30 Felber, R., Münger, A., Neftel, A. and Ammann, C.: Eddy covariance methane flux measurements over a grazed pasture: effect  
31 of cows as moving point sources, *Biogeosciences*, 12(12), 3925–3940, doi:10.5194/bg-12-3925-2015, 2015.
- 32 Flechard, C. R. and Sutton, M. A.: Advances in understanding, models and parameterizations of biosphere-atmosphere  
33 ammonia exchange, , 43, 2013.

- 1 Flesch, T. K., Wilson, J. D., Harper, L. A., Crenna, B. P. and Sharpe, R. R.: Deducing Ground-to-Air Emissions from Observed  
2 Trace Gas Concentrations: A Field Trial, *J. Appl. Meteorol.*, 43(3), 487–502, doi:10.1175/1520-  
3 0450(2004)043<0487:DGEFOT>2.0.CO;2, 2004.
- 4 Flesch, T. K., Wilson, J. D. and Harper, L. A.: Deducing ground-to-air emissions from observed trace gas concentrations: a  
5 field trial with wind disturbance, *J. Appl. Meteorol.*, 44(4), 475–484, 2005.
- 6 Flesch, T. K., McGinn, S. M., Chen, D., Wilson, J. D. and Desjardins, R. L.: Data filtering for inverse dispersion emission  
7 calculations, *Agric. For. Meteorol.*, 198–199, 1–6, doi:10.1016/j.agrformet.2014.07.010, 2014.
- 8 Häni, C.: bLSmodelR – An atmospheric dispersion model in R. [online] Available from: [http://www.agrammon.ch/  
9 documents-to-download/blsmodelr/](http://www.agrammon.ch/documents-to-download/blsmodelr/) (Accessed 24 October 2017), 2017.
- 10 Häni, C., Sintermann, J., Kupper, T., Jocher, M. and Neftel, A.: Ammonia emission after slurry application to grassland in  
11 Switzerland, *Atmos. Environ.*, 125, 92–99, doi:10.1016/j.atmosenv.2015.10.069, 2016.
- 12 Häni, C., Flechard, C., Neftel, A., Sintermann, J. and Kupper, T.: Accounting for Field-Scale Dry Deposition in Backward  
13 Lagrangian Stochastic Dispersion Modelling of NH<sub>3</sub> Emissions, , doi:10.20944/preprints201803.0026.v1, 2018.
- 14 Harper, L. A., Flesch, T. K., Weaver, K. H. and Wilson, J. D.: The Effect of Biofuel Production on Swine Farm Methane and  
15 Ammonia Emissions, *J. Environ. Qual.*, 39(6), 1984–1992, doi:10.2134/jeq2010.0172, 2010.
- 16 Jarvis, S. C., Hatch, D. J. and Roberts, D. H.: The effects of grassland management on nitrogen losses from grazed swards  
17 through ammonia volatilization; the relationship to excretal N returns from cattle, *J. Agric. Sci.*, 112(02), 205,  
18 doi:10.1017/S0021859600085117, 1989.
- 19 Jiang, Y., Deng, A., Bloszies, S., Huang, S. and Zhang, W.: Nonlinear response of soil ammonia emissions to fertilizer nitrogen,  
20 *Biol. Fertil. Soils*, 53(3), 269–274, doi:10.1007/s00374-017-1175-3, 2017.
- 21 Kumar, A., Sharifi, H. and Arif, K. M.: Mobile machine vision development for urine patch detection, pp. 1–6, *IEEE.*, 2016.
- 22 Kupper, T., Bonjour, C. and Menzi, H.: Evolution of farm and manure management and their influence on ammonia emissions  
23 from agriculture in Switzerland between 1990 and 2010, *Atmos. Environ.*, 103, 215–221,  
24 doi:10.1016/j.atmosenv.2014.12.024, 2015.
- 25 Laubach, J., Taghizadeh-Toosi, A., Sherlock, R. R. and Kelliher, F. M.: Measuring and modelling ammonia emissions from a  
26 regular pattern of cattle urine patches, *Agric. For. Meteorol.*, 156, 1–17, doi:10.1016/j.agrformet.2011.12.007, 2012.
- 27 Laubach, J., Bai, M., Pinares-Patiño, C. S., Phillips, F. A., Naylor, T. A., Molano, G., Rocha, E. A. C. and Griffith, D. W.:  
28 Accuracy of micrometeorological techniques for detecting a change in methane emissions from a herd of cattle, *Agric. For.  
29 Meteorol.*, 176, 50–63, 2013a.
- 30 Laubach, J., Taghizadeh-Toosi, A., Gibbs, S. J., Sherlock, R. R., Kelliher, F. M. and Grover, S. P. P.: Ammonia emissions  
31 from cattle urine and dung excreted on pasture, *Biogeosciences*, 10(1), 327–338, doi:10.5194/bg-10-327-2013, 2013b.
- 32 Luo, J., Wyatt, J., van der Weerden, T. J., Thomas, S. M., de Klein, C. A. M., Li, Y., Rollo, M., Lindsey, S., Ledgard, S. F.,  
33 Li, J., Ding, W., Qin, S., Zhang, N., Bolan, N., Kirkham, M. B., Bai, Z., Ma, L., Zhang, X., Wang, H., Liu, H. and Rys, G.:

- 1 Potential Hotspot Areas of Nitrous Oxide Emissions From Grazed Pastoral Dairy Farm Systems, in *Advances in Agronomy*,  
2 vol. 145, pp. 205–268, Elsevier., 2017.
- 3 McGinn, S. M., Beauchemin, K. A., Flesch, T. K. and Coates, T.: Performance of a Dispersion Model to Estimate Methane  
4 Loss from Cattle in Pens, *J. Environ. Qual.*, 38(5), 1796, doi:10.2134/jeq2008.0531, 2009.
- 5 MeteoSwiss: Climate normals Fribourg/Posieux, [online] Available from:  
6 [www.meteoschweiz.admin.ch/product/output/climate-data/climate-diagrams-normal-values-station-](http://www.meteoschweiz.admin.ch/product/output/climate-data/climate-diagrams-normal-values-station-processing/GRA/climsheet_GRA_np8110_e.pdf)  
7 [processing/GRA/climsheet\\_GRA\\_np8110\\_e.pdf](http://www.meteoschweiz.admin.ch/product/output/climate-data/climate-diagrams-normal-values-station-processing/GRA/climsheet_GRA_np8110_e.pdf) (Accessed 31 January 2018), 2018.
- 8 Misselbrook, T., Fleming, H., Camp, V., Umstatter, C., Duthie, C.-A., Nicoll, L. and Waterhouse, T.: Automated monitoring  
9 of urination events from grazing cattle, *Agric. Ecosyst. Environ.*, 230, 191–198, doi:10.1016/j.agee.2016.06.006, 2016.
- 10 Misselbrook, T. H., Nicholson, F. A. and Chambers, B. J.: Predicting ammonia losses following the application of livestock  
11 manure to land, *Bioresour. Technol.*, 96(2), 159–168, doi:10.1016/j.biortech.2004.05.004, 2005.
- 12 Móríng, A., Vieno, M., Doherty, R. M., Laubach, J., Taghizadeh-Toosi, A. and Sutton, M. A.: A process-based model for  
13 ammonia emission from urine patches, *GAG (Generation of Ammonia from Grazing): description and sensitivity analysis*,  
14 *Biogeosciences*, 13(6), 1837–1861, doi:10.5194/bg-13-1837-2016, 2016.
- 15 Móríng, A., Vieno, M., Doherty, R. M., Milford, C., Nemitz, E., Twigg, M. M., Horváth, L. and Sutton, M. A.: Process-based  
16 modelling of NH<sub>3</sub> exchange with grazed grasslands, *Biogeosciences*, 14(18), 4161–4193, doi:10.5194/bg-14-4161-2017,  
17 2017.
- 18 Munger, J. W., Loescher, H. W. and Luo, H.: Measurement, Tower, and Site Design Considerations, in *Eddy Covariance: A*  
19 *Practical Guide to Measurement and Data Analysis*, edited by M. Aubinet, T. Vesala, and D. Papale, pp. 21–58, Springer  
20 Netherlands, Dordrecht., 2012.
- 21 Nemitz, E., Dorsey, J. R., Flynn, M. J., Gallagher, M. W., Hensen, A., Erismann, J.-W., Owen, S. M., Dämmgen, U. and Sutton,  
22 M. A.: Aerosol fluxes and particle growth above managed grassland, *Biogeosciences*, 6(8), 1627–1645, doi:10.5194/bg-6-  
23 1627-2009, 2009.
- 24 Peltola, O., Hensen, A., Beletti Marchesini, L., Helfter, C., Bosveld, F. C., van den Bulk, W. C. M., Haapanala, S., van  
25 Huissteden, J., Laurila, T., Lindroth, A., Nemitz, E., Röckmann, T., Vermeulen, A. T. and Mammarella, I.: Studying the spatial  
26 variability of methane flux with five eddy covariance towers of varying height, *Agric. For. Meteorol.*, 214–215(Supplement  
27 C), 456–472, doi:10.1016/j.agrformet.2015.09.007, 2015.
- 28 Petersen, S. O., Sommer, S. G., Aaes, O. and Sørensen, K.: Ammonia losses from urine and dung of grazing cattle: effect of  
29 N intake, *Atmos. Environ.*, 32(3), 295–300, doi:10.1016/S1352-2310(97)00043-5, 1998.
- 30 Quin, B., Bates, G. and Bishop, P.: LOCATING AND TREATING FRESH COW URINE PATCHES WITH SPIKEY®; THE  
31 PLATFORM FOR PRACTICAL AND COST-EFFECTIVE REDUCTION IN ENVIRONMENTAL N LOSSES, *Integr. Nutr.*  
32 *Water Manag. Sustain. FarmingEds LD Currie R Singh Httpflrc Massey Ac Nzpublications Html Occas. Rep.*, (29), 2016.
- 33 R Core Team: R: A Language and Environment for Statistical Computing, R Foundation for Statistical Computing, Vienna,  
34 Austria. [online] Available from: <https://www.R-project.org/>, 2016.

- 1 Sintermann, J., Neftel, A., Ammann, C., Häni, C., Hensen, A., Loubet, B. and Flechard, C. R.: Are ammonia emissions from  
2 field-applied slurry substantially over-estimated in European emission inventories?, *Biogeosciences*, 9(5), 1611–1632,  
3 doi:10.5194/bg-9-1611-2012, 2012.
- 4 Sintermann, J., Dietrich, K., Häni, C., Bell, M., Jocher, M. and Neftel, A.: A miniDOAS instrument optimised for ammonia  
5 field-measurements, *Atmospheric Meas. Tech. Discuss.*, 1–26, doi:10.5194/amt-2015-360, 2016.
- 6 Sommer, S. G. and Olesen, J. E.: Modelling ammonia volatilization from animal slurry applied with trail hoses to cereals,  
7 *Atmos. Environ.*, 34(15), 2361–2372, 2000.
- 8 Sutton, M. A., Howard, C. M., Erisman, J. W., Bealey, W. J., Billen, G., Bleeker, A., Bouwman, A. F., Grennfelt, P., van  
9 Grinsven, H. and Grizzetti, B.: The challenge to integrate nitrogen science and policies: the European Nitrogen Assessment  
10 approach, in *The European Nitrogen Assessment: Sources, Effects and Policy Perspectives*, edited by A. Bleeker, B. Grizzetti,  
11 C. M. Howard, G. Billen, H. van Grinsven, J. W. Erisman, M. A. Sutton, and P. Grennfelt, pp. 82–96, Cambridge University  
12 Press, Cambridge., 2011.
- 13 **Voglmeier, K., Jocher, M., Häni, C. and Ammann, C.: Ammonia emission measurements of an intensively grazed pasture -  
14 Dataset., 2018.**
- 15 Volten, H., Bergwerff, J. B., Haaima, M., Lolkema, D. E., Berkhout, A. J. C., van der Hoff, G. R., Potma, C. J. M., Wichink  
16 Kruit, R. J., van Pul, W. A. J. and Swart, D. P. J.: Two instruments based on differential optical absorption spectroscopy  
17 (DOAS) to measure accurate ammonia concentrations in the atmosphere, *Atmos Meas Tech*, 5(2), 413–427, doi:10.5194/amt-  
18 5-413-2012, 2012.
- 19 Yan, T., Frost, J. P., Agnew, R. E., Binnie, R. C. and Mayne, C. S.: Relationships among manure nitrogen output and dietary  
20 and animal factors in lactating dairy cows, *J. Dairy Sci.*, 89(10), 3981–3991, 2006.

21  
22  
23  
24  
25  
26  
27  
28  
29  
30  
31  
32  
33  
34

1 **Table 1: Summary of grazing rotations 2016 on paddocks X.11 and X.12 investigated for NH<sub>3</sub> emissions**

Rotation no.	Start date	Sojourn time on pasture [h]	Sojourn time in barn [h]
1	2016-05-09	44.5	11
2	2016-05-26	46.5	9
3	2016-07-04	37	8.5
4	2016-07-26	51	20.5
5	2016-08-10	29	8
6	2016-09-04	36.5	17
7	2016-09-26	55	13

2

3

4

5

6

7

8

9

10

11

12

13

14

15

16

17

18

19

20

21

22

23

24

1 **Table 2: Measured driving parameters and resulting urine N and feces N of the animal N budget model averaged for the individual**  
 2 **rotations and for each herd (system M / G). If only one number is given it corresponds to both herds simultaneously. Rotation 4 is**  
 3 **not shown due to missing miniDOAS measurements.**

Rotation	1	2	3	5	6	7
System	M   G	M   G	M   G	M   G	M   G	M   G
Animal weight (kg)	639   635	646   635	636   637	630   630	630   637	633   637
Days since calving	187   199	204   216	182   197	217   218	242   243	258   265
Milk yield (kg cow <sup>-1</sup> d <sup>-1</sup> )	26.7   25.3	24.4   23.7	25.0   23.8	23.3   23.3	23.2   20.6	19.2   15.9
Grass crude protein (g kg-DM <sup>-1</sup> )	203	147	178	200	218	200
Maize crude protein (g kg-DM <sup>-1</sup> )	91   <i>na</i>	91   <i>na</i>	89   <i>na</i>	80   <i>na</i>	72   <i>na</i>	71   <i>na</i>
Urine N (g cow <sup>-1</sup> d <sup>-1</sup> )	274   324	135   157	218   269	266   326	295   371	244   317
Feces N (g cow <sup>-1</sup> d <sup>-1</sup> )	160   157	146   146	150   152	150   151	153   149	147   142

4  
5  
6  
7  
8  
9  
10  
11  
12  
13  
14  
15  
16  
17  
18

1 **Table 3: Cumulative emission results for paddocks X.11 and X.12 (combined) of the two pasture systems (M / G) during the**  
 2 **individual rotations. Corresponding averaged weather parameters and N excretion input to the paddocks are also listed. Rotation 4**  
 3 **is not shown due to missing miniDOAS data at the beginning of the rotation.**

Rotation	1	2	3	5	6	7
System	M   G	M   G	M   G	M   G	M   G	M   G
flux data coverage (until 3 days after EOG) [%]	55   <i>na</i>	65   44	34   39	<i>na</i>   30	50   <i>na</i>	51   50
Air temperature [°C]	11.9	14.8	18.9	17.8	18.1	14.4
u* [m s <sup>-1</sup> ]	0.13	0.15	0.12	0.09	0.11	0.13
Precipitation [mm]	51	75	61	7	33	10
Integral emission [g N-NH <sub>3</sub> ]	332   <i>na</i>	349   600	357   496	<i>na</i>   341	277   <i>na</i>	330   726
N excretion total [kg]	9.6   10.7	6.5   7.1	6.8   7.8	5.9   6.9	8.2   9.5	10.8   12.6
N excretion urine [kg]	6.1   7.2	3.1   3.6	4.0   5.0	3.8   4.7	5.4   6.7	6.7   8.7
EF relative to urine N input [%]	5.5   <i>na</i>	11.1   16.4	8.8   10.0	<i>na</i>   7.2	5.1   <i>na</i>	4.9   8.3

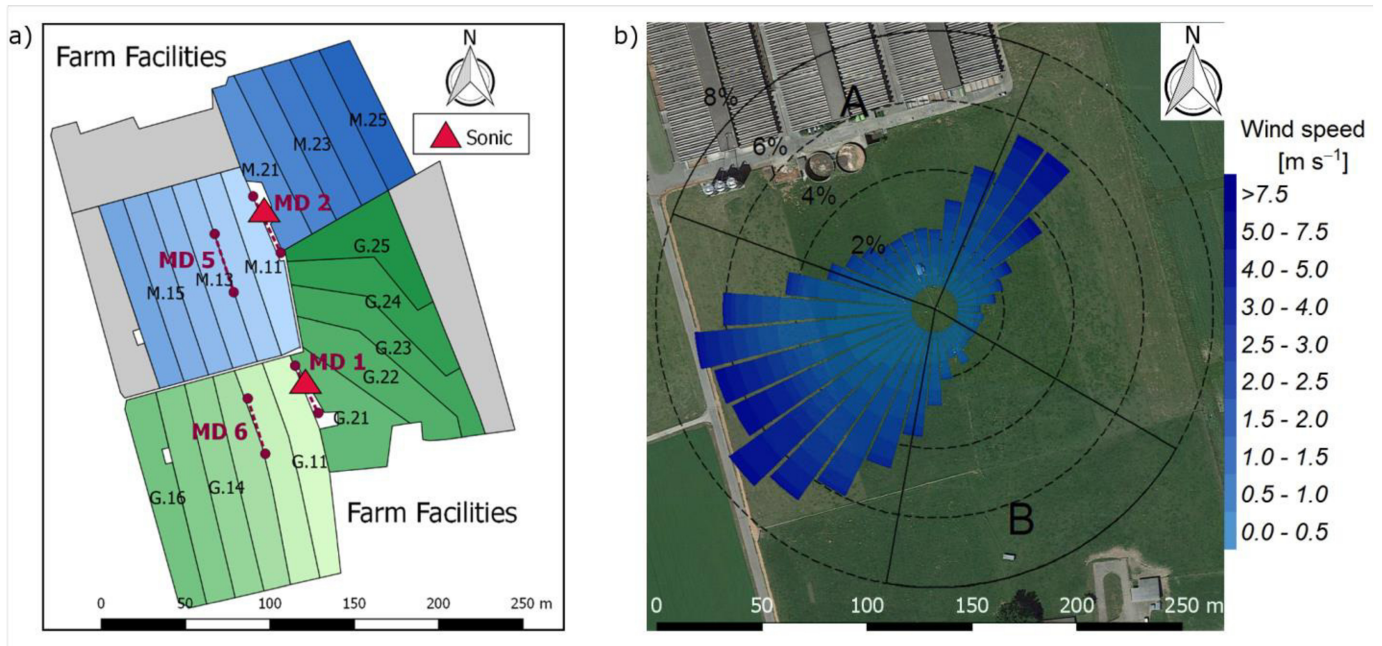
4  
5  
6  
7  
8  
9  
10  
11  
12  
13  
14  
15



1 **Table 4: Artificial source characteristics, environmental conditions, measured MD concentrations and recovery rates during the**  
 2 **individual gas release experiments. Averaged values during the release periods are shown. For selected parameters, the standard**  
 3 **deviation is given as well.**

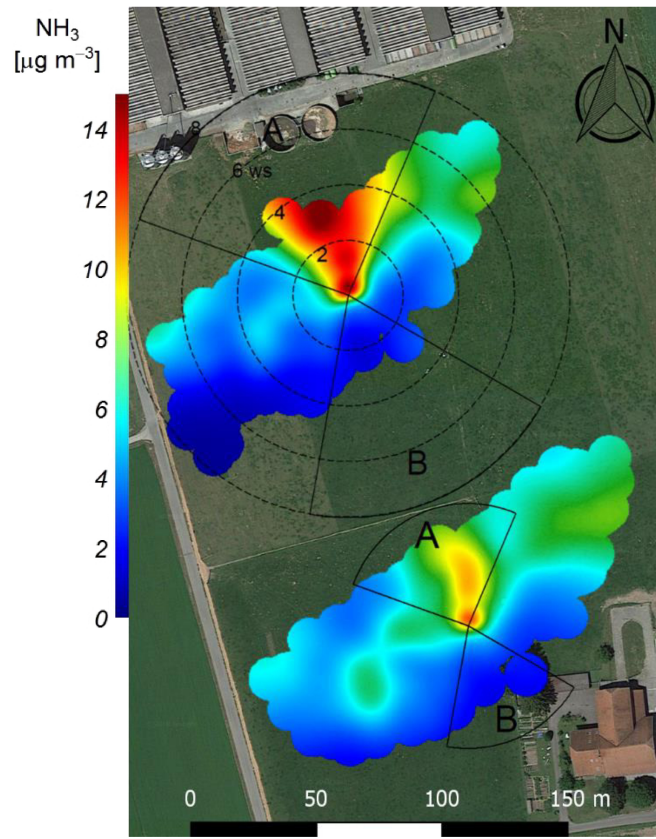
Release date	09-06-2017	12-06-2017	19-06-2017	27-06-2017	12-07-2017
Parameter					
Release duration [h]	1.5	2.5	3.5	1.5	3.0
Pressure [bar]	5.48±1.15	5.14±0.1	3.57±0.51	5.05±0.07	4.68±0.29
Flowrate [l/min]	3.12 ± 0.08	3.12 ± 0.07	2.59 ± 0.34	3.17 ± 0.04	3.13 ± 0.06
Abs. Emission [g NH <sub>3</sub> ]	10.6	17.8	20.7	10.8	21.0
Wind direction [°]	269	272	256	230	240
Friction velocity [m s <sup>-1</sup> ]	0.18 ± 0.04	0.26 ± 0.03	0.25 ± 0.04	0.26 ± 0.07	0.53 ± 0.05
Air temperature [°C]	20.1	25.6	26.0	24.6	24.1
ΔC [μg NH <sub>3</sub> m <sup>-3</sup> ]	40.6 ± 10.3	29.5 ± 9.1	14.3 ± 4.9	26.4 ± 7.1	9.4 ± 2.3
Upwind conc. [μg NH <sub>3</sub> m <sup>-3</sup> ]	2.2 ± 1.9	3.3 ± 2.5	15.3 ± 1.4	6.6 ± 1.7	1.2 ± 0.3
Recovery rate [%]	150 ± 4	124 ± 10	88 ± 9	114 ± 9	112 ± 12

4  
5  
6  
7  
8  
9  
10  
11  
12  
13



1  
2  
3  
4  
5  
6  
7  
8  
9  
10  
11  
12  
13  
14  
15  
16  
17  
18  
19  
20  
21  
22

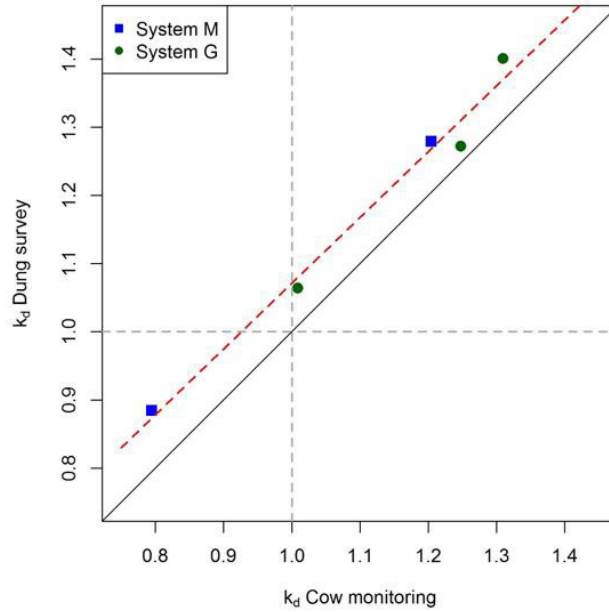
Figure 1: a) Measurement site with the pastures for the two herds (blue: grass diet with additional maize silage; green: full grazing regime; grey: optional pasture areas) and the division into the paddocks (M.11-M.25, G.11-G.25). Additionally the location of the two sonic anemometers and the four miniDOAS systems (MD1 – MD6, naming based on serial number) are shown. b) Wind distribution for the northern sonic anemometer with the corresponding sector contributions (black dotted circles) for the period May – October 2016. The areas A and B indicate wind sectors from which advection from nearby farm building can occur. The wind distribution was overlaid on a Google Earth image of the experimental area (Map data: Google, DigitalGlobe)



1

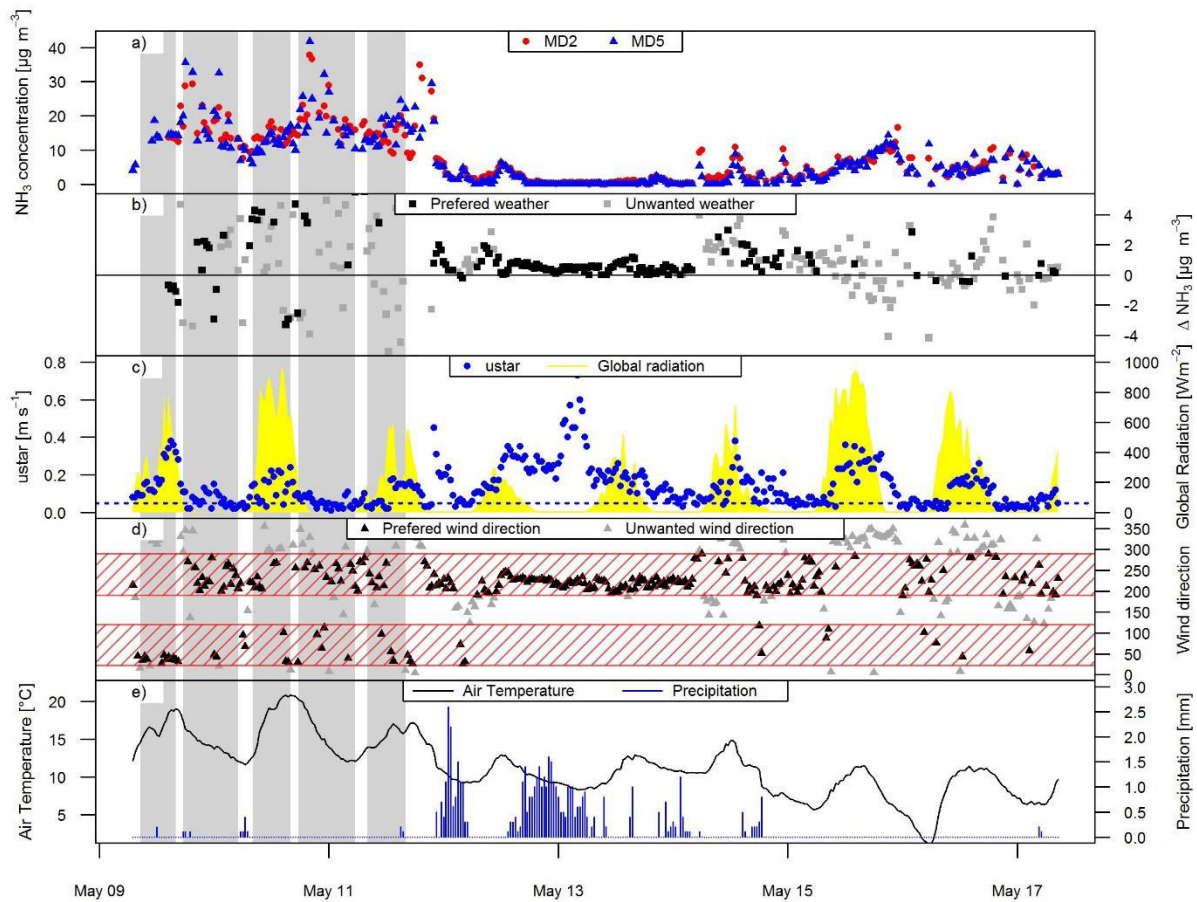
2 **Figure 2: The Polar plot shows the averaged NH<sub>3</sub> concentration of the miniDOAS MD5 (top) and MD6 (bottom) depending on wind**  
 3 **direction and wind speed (black dotted circles) for the period May – October 2016. The sectors A and B indicate areas with either**  
 4 **high NH<sub>3</sub> concentration from farm buildings or otherwise unfavourable wind direction due to the measurement setup. The polar**  
 5 **plots were produced using the R software package openair (Carslaw and Ropkins, 2012) and overlaid on a Google Earth image of**  
 6 **the experimental area (Map data: Google, DigitalGlobe).**

7



b)

Figure 3: (a) GPS tagged dung positions recorded after grazing rotation 7 overlaid on a Google Earth image of the experimental area (Map data: Google, DigitalGlobe). The positions of the MD ammonia sensors/paths are indicated by the red dots/dotted lines. The white lines enclose the main emission measurement area between the sensors. Their dung patch density  $d_{X,meas}$  was related to the average density over the investigated paddocks according to Eq. 2; (b) comparison of  $k_d$  values according to Eq. 2 for dung patch and cow position distributions on system M (blue) and system G (green)



1

2 **Figure 4:** Time series of a) MD concentration measurements (MD2 and MD5) ~~of~~ **on** pasture system M and b) corresponding  
 3 difference in concentration. The concentration differences during good wind conditions are shown in black colour while the grey  
 4 colour indicate concentration differences during undesirable weather conditions. c) Time series of  $u^*$  and global radiation. The blue  
 5 dashed line indicate the  $0.05 \text{ m s}^{-1} u^*$  threshold. d) Time series of wind direction. Wind direction values overlapping with the  
 6 preferred wind sector (avoiding sector A and B, ~~see~~ Fig. 2) are shown in black colour. The preferred wind sectors are indicated by  
 7 the red area. e) Time series of air temperature and precipitation. The grey shaded area indicates grazing on the paddocks in between  
 8 MD2 and MD5.

9

10

11

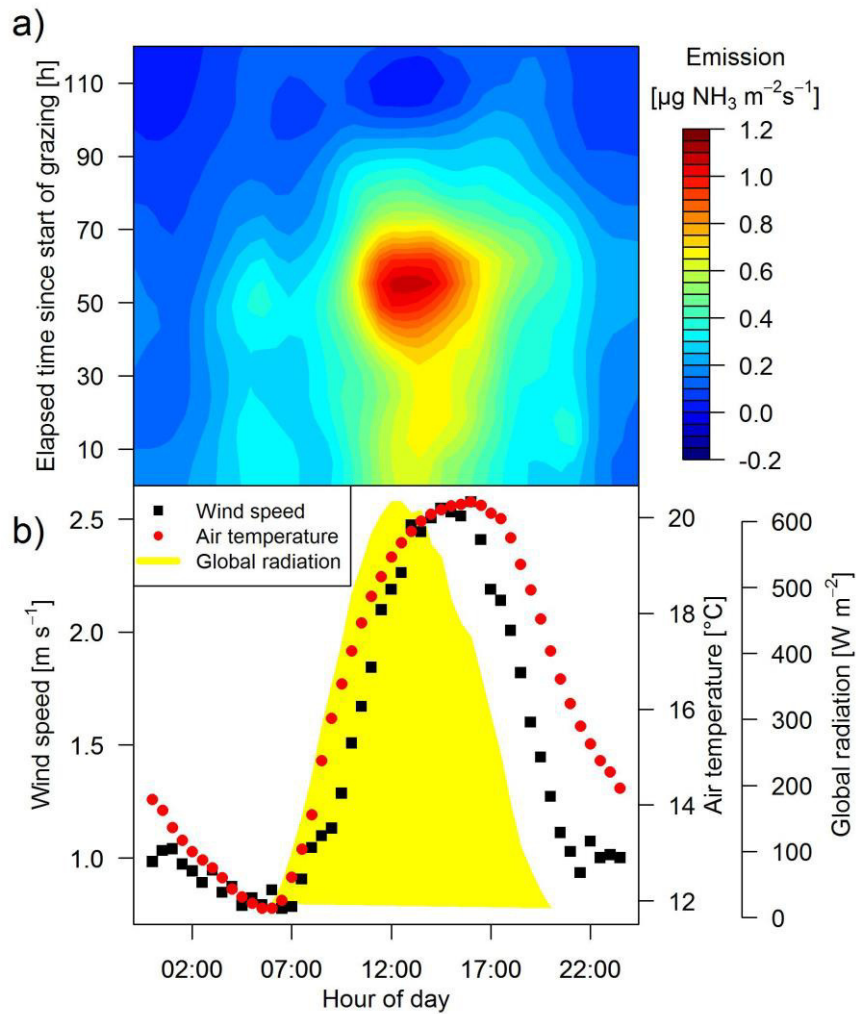
12

13

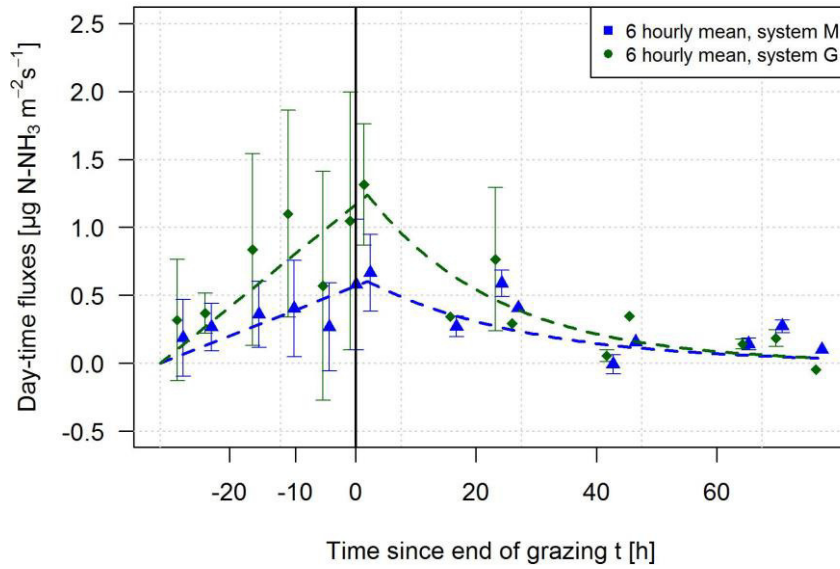
14

15

16



1  
 2 **Figure 5:** a) Measured averaged half hourly fluxes of all rotations of the system M depending on hour of day and elapsed time since  
 3 grazing on the paddocks in between MD2 and MD5 started. b) Half hourly averaged values of global radiation, wind speed and air  
 4 temperature measured at system M during May to October 2016.



1

2 **Figure 6: Average temporal pattern of management related NH<sub>3</sub> emission for system M (blue) and system G (green) for daytime**  
 3 **conditions. Curves with linear increase from start of grazing until three hours after end of grazing and exponential decrease**  
 4 **afterwards were fitted to the 6-hourly averaged values of the measured daytime fluxes. These curves were used as default emission**  
 5 **pattern for flux correction and gap filling (see Section 3.2). The curves were used as default emission**  
 6 **pattern for flux correction and gap filling (see Section 3.2). The vertical bars indicate the standard deviation of averaged half-hourly**  
 7 **fluxes. The black vertical line indicates the end of grazing. For better readability the data points for the two systems were slightly**  
 8 **shifted horizontally.**

8

9

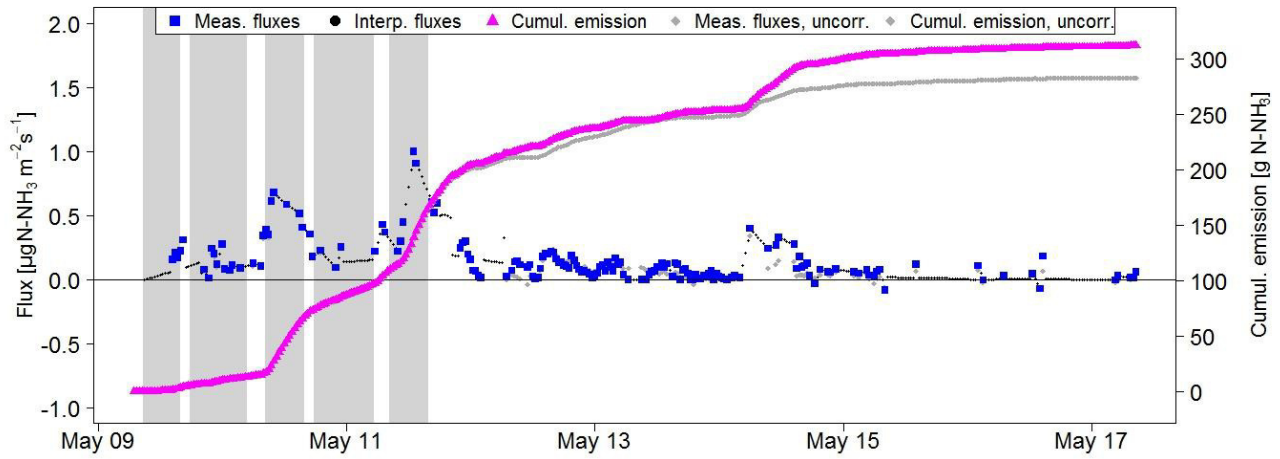
10

11

12

13

14



1

2

**Figure 7:** Measured emission of paddocks M.11 and M.12 (between sensors MD2 and MD5, Fig. 1a) during rotation 1. Missing half-hourly flux data were filled based on either linear interpolation or on the default emission curve (Fig. 6) in order to compute the cumulative emission. For comparison the uncorrected emissions (interference of upwind grazing acc. to Eq. 4 not considered) are also shown. The shaded time intervals indicate grazing on the investigated paddocks.

6

7

8

9

10

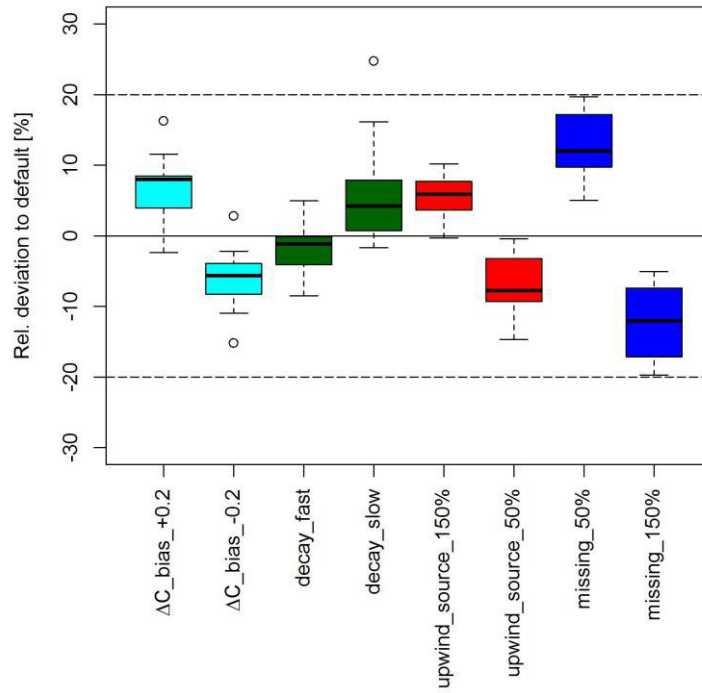
11

12

13

14





1

2 **Figure 8:** Sensitivity analysis of various error sources on emission results for individual rotations. Each boxplot shows the resulting  
 3 relative effect of a potential systematic error. The investigated effects include the over- or underestimation of: the offset in  
 4 concentration measurements (cyan), exponential decay times of the **default** emission curves in Fig. 6 (green), magnitude of **default**  
 5 emission curves used for upwind source interference correction (red) and for gap filling (blue).

6

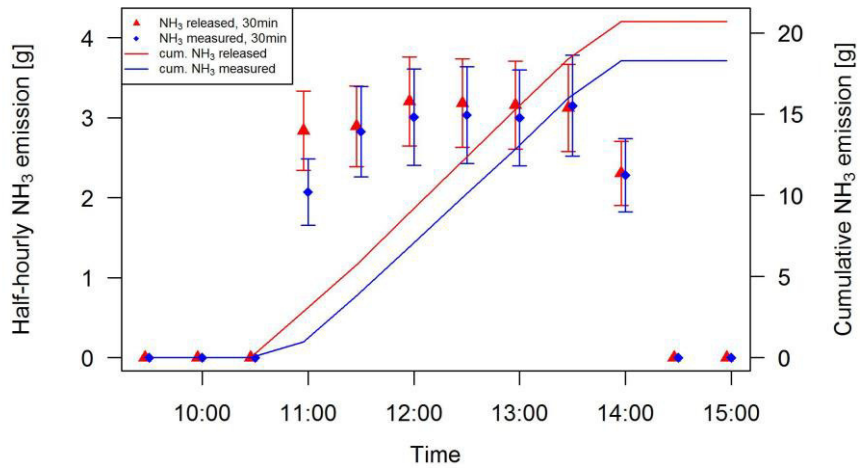
7

8

9

10

11



1

2 **Figure 9: Released (red) and measured (blue) NH<sub>3</sub> emissions during the artificial source experiment 3 on the 19 June 2017. The**  
 3 **measured emissions were quantified using the concentration difference of the miniDOAS systems MD2 and MD5 and the**  
 4 **corresponding modelled bLS dispersion coefficient. The error bars indicate the uncertainty of the artificial source (Sect. 3.3.2) and**  
 5 **from the measured emissions (bLS dispersion modelling, Sect. 3.3).**

6

7

8

9

10

11

12

13

14

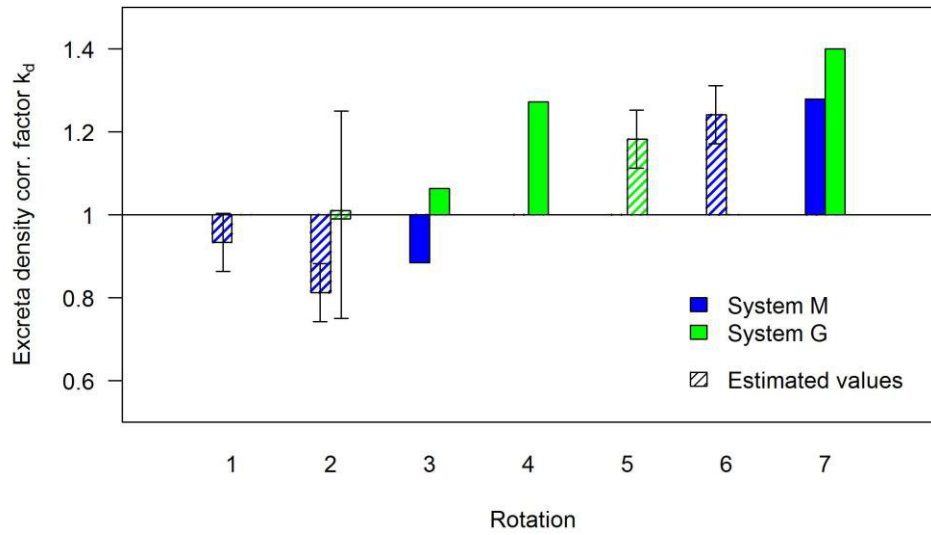
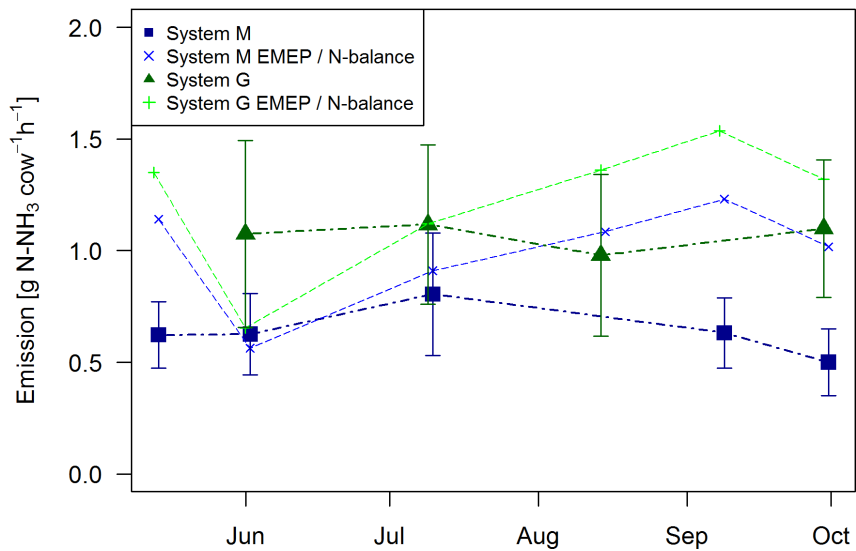


**Figure 10:** Correction factor  $k_d$  (Eq. 2, 3) of the excreta density for rotations with available emission results (Table 3). For the rotations without dung observations, the corresponding correction factors (hatched bars) were estimated based on a regression analysis between parallel surveys of density anomalies for dung patches and cow positions (Fig. 3b). The error bars show the corresponding uncertainty of estimated  $k_d$  values as described in Sect. 3.4.



1

2 **Figure 11: Emissions per cow and grazing hour for system M and system G. Measured values (thick dots and lines) in comparison**  
 3 **to estimated values based on urine N amount from the N balance model and the EMEP standard emission factor for  $\text{NH}_3$  (10 %, see**  
 4 **EMEP/EEA, 2016). The error bars ( $2\sigma$ ) were calculated based on the methodological uncertainty (Sect. 3.3.1) and on excreta density**  
 5 **uncertainty of the single rotations (Sect. 3.4).**

6